A General Framework for Learning from Weak Supervision

Anonymous Authors[1]

Abstract

Weakly supervised learning generally faces challenges in applicability to various scenarios with diverse weak supervision and in scalability due to the complexity of existing algorithms, thereby hindering the practical deployment. This paper introduces a general framework for learning from weak supervision (GLWS) with a novel algorithm. Central to GLWS is an Expectation-Maximization (EM) formulation, adeptly accommodating various weak supervision sources, including instance partial labels, aggregate statistics, pairwise observations, and unlabeled data. We further present an advanced algorithm that significantly simplifies the EM computational demands using a Non-deterministic Finite Automaton (NFA) along with a forward-backward algorithm, which effectively reduces time complexity from quadratic or factorial often required in existing solutions to linear scale. The problem of learning from arbitrary weak supervision is therefore converted to the NFA modeling of them. GLWS not only enhances the scalability of machine learning models but also demonstrates superior performance and versatility across 11 weak supervision scenarios. We hope our work paves the way for further advancements and practical deployment in this field.

1. Introduction

Over the past few years, machine learning models have shown promising performance in virtually every aspect of our lives (Radford et al., 2021; Rombach et al., 2022; Dehghani et al., 2023; OpenAI, 2023). This success is typically attributed to large-scale and high-quality training data with complete and accurate supervision. However, obtaining such precise labels in realistic applications is often prohibitive due to various factors, such as the cost of annotation (Settles et al., 2008; Gadre et al., 2023), the biases and subjectivity of annotators (Tommasi et al., 2017; Pagano et al., 2023), and privacy concerns (Mireshghallah et al., 2020; Strobel & Shokri, 2022). The resulting *incomplete*, *inexact*, and *inaccurate* forms of supervision are typically referred to as *weak supervision* (Zhou, 2018; Sugiyama et al., 2022).

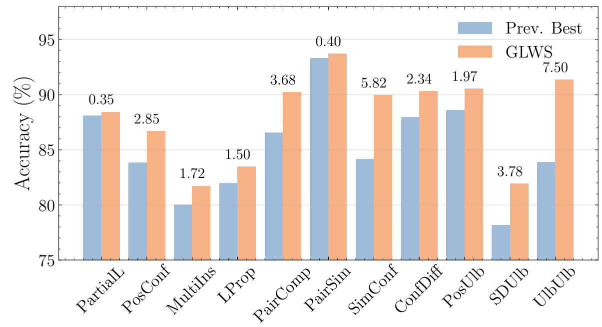

Figure 1. Average performance overview of the proposed method on 11 common weak supervision settings, compared to previous best methods (margins shown on the top of bars). GLWS is capable of learning from any weak supervision universally and effectively.

Previous literature has explored numerous configurations of weak supervision problems, including learning from sets of instance label candidates (Luo & Orabona, 2010; Cour et al., 2011; Ishida et al., 2019; Feng et al., 2020a;c; Wang et al., 2022a; Wu et al., 2022), aggregate group statistics (Maron & Lozano-Pérez, 1997; Zhou, 2004; Kück & de Freitas, 2005; Quadrianto et al., 2008; Ilse et al., 2018; Zhang et al., 2020; Scott & Zhang, 2020; Zhang et al., 2022), pairwise observations (Bao et al., 2018; 2020; Feng et al., 2021; Cao et al., 2021b; Wang et al., 2023a), and unlabeled data (Lu et al., 2018; Sohn et al., 2020; Shimada et al., 2021; Wang et al., 2022b; Tang et al., 2023). More recently, some efforts have been made to design versatile techniques that can handle multiple settings simultaneously (Van Rooyen & Williamson, 2018; Zhang et al., 2020; Chiang & Sugiyama, 2023; Shukla et al., 2023; Wei et al., 2023).

Despite the prosperous developments in various settings, we identify two challenges that impede the practical application of these weakly supervised methods. First, designing a method capable of universally handling all configurations remains difficult. The variation in forms of weak supervision often necessitates specialized and tailored solutions (Ilse et al., 2018; Yan et al., 2018; Yang et al., 2022; Zhang et al., 2022; Scott & Zhang, 2020). Even recent versatile solutions

[1]Anonymous Institution, Anonymous City, Anonymous Region, Anonymous Country. Correspondence to: Anonymous Author <anon.email@domain.com>.

Preliminary work. Under review by the International Conference on Machine Learning (ICML). Do not distribute.

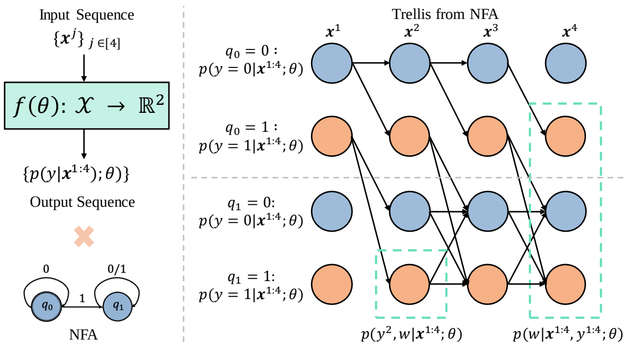

Figure 2. Overview of GLWS for learning from arbitrary weak supervision. We model weak supervision as a Non-deterministic Finite Automaton (NFA). By taking the product of the prediction sequence and NFA, we can utilize the forward-backward algorithm to solve the proposed complete EM formulation in linear time.

are limited in their applicability to certain contexts (Shukla et al., 2023; Wei et al., 2023). Second, prior works typically exhibit limited scalability in realistic problems due to oversimplifications and unfavorable modeling complexity. Some methods assume conditional independence of instances for aggregate observations (Van Rooyen & Williamson, 2018; Cui et al., 2020; Zhang et al., 2020; Wei et al., 2023), making them unsuitable for handling long sequence data prevalent in practical scenarios. Moreover, despite such simplifications, they still require infeasible computational complexity, either quadratic (Shukla et al., 2023) or factorial (Wei et al., 2023), to address specific weak supervision configurations.

To overcome these challenges and effectively apply weakly supervised learning in real-world scenarios, we propose a general framework and a novel algorithm that allows efficient learning from arbitrary weak supervision, termed as GLWS, as in the results demonstrated in Fig. 1. At the core of GLWS is an Expectation-Maximization (EM) (Dempster et al., 1977) learning objective formulation for weak supervision, and a forward-backward algorithm (Rabiner, 1989; Graves et al., 2006) designed to solve the EM in linear time by representing arbitrary form of weak supervision as a Non-deterministic Finite Automaton (NFA) (Rabin & Scott, 1959). More specifically, to train a classification model with learnable parameters θ on weak supervision, denoted abstractly as W, we treat the ground truth label Y as a missing latent variable and maximize the log-likelihood of joint input X and W: $\log P(X, W; \theta) = \log \sum_Y P(X, W; \theta) P(Y|X, W; \theta)$. As $P(Y|X, W; \theta)$ is unknown before determining θ, solving the problem usually requires iterative hill-climbing solutions. Therefore, we employ the widely used EM algorithm, which iteratively maximizes the expectation of the log-likelihood $\mathbb{E}_{Y|X,W;\theta^t}[\log P(X, W, Y; \theta)]$ at time step t. It leads to two training objectives: an unsupervised instance consistency term $\mathbb{E}_{Y|X,W;\theta^t}[\log P(Y|X; \theta)]$ that encourages the prediction to be consistent with the labeling distribution imposed by W, and a supervised objective $\log P(W|Y, X; \theta)$ that fosters the group predictions fulfilling W. We further propose a novel perspective to perform the EM formulation. Without loss of generality, we treat both the inputs and the precise labels as sequence[1]. Thus, the problem of identifying all possible labelings is converted into assigning labels/symbols to the input sequence in a manner that adheres to W. This process can be effectively modeled using an NFA (Rabin & Scott, 1959), where the finite set of states and transition is dictated by W, and the finite set of symbols corresponds to Y. The EM learning objectives can then be computed efficiently in linear time using a forward-backward algorithm on the *trellis* expanded from the NFA and model's predictions. An overview is shown in Fig. 2.

While this is not the first EM perspective of weak supervision (Denœux, 2011; Quost & Denoeux, 2016; Wang et al., 2022a; Wei et al., 2023), GLWS distinguishes from prior arts in solving the *complete EM efficiently and practically*. Compared to the recent efforts towards the unification of weak supervision, our method neither relies on the aforementioned conditional independence assumption as in Wei et al. (2023) nor involves approximation of EM as in Wang et al. (2022a); Shukla et al. (2023) that solves the supervised term of EM only. Our contributions can be summarized as:

- We propose an EM framework that accommodates weak supervision of arbitrary forms, leading to two learning objectives, as a generalization of the prior arts.
- We design a forward-backward algorithm that performs the EM by treating weak supervision as an NFA. The EM can thus be computed via iterative forward-backward pass on the trellis expanded from the NFA in linear time.
- On **11** weak supervision settings, the proposed method consistently achieves the state-of-the-art performance, demonstrating its universality and effectiveness. The codebase covering all these settings will be released.

2. Related Work

2.1. Learning from Weak Supervision

Various problems for learning from weak supervision have been extensively studied in the past, and we categorize them into four broad categories: instance label candidates, aggregate observations, pairwise observations, and unlabeled data. Learning from instance label candidates, also known as partial label (PartialL) or complementary label (CompL) learning (Cour et al., 2011; Luo & Orabona, 2010; Feng et al., 2020b; Wang et al., 2019; Wen et al., 2021; Wu et al., 2022;

[1]For aggregate and pairwise observations, the inputs are naturally sequences of instances. The inputs can be viewed as permutation-invariant sequences at the batch (dataset) level for weak supervision of partial labels and unlabeled data. The same applies to the precise labels and predictions from the model.

Wang et al., 2022a; Ishida et al., 2019; Feng et al., 2020a), involves weak supervision as a set of label candidates, either containing or complementary to the ground truth label for each instance. Aggregate observation assumes supervision over a group of instances (Zhang et al., 2020), with multiple instances (MultiIns) learning (Maron & Lozano-Pérez, 1997; Ilse et al., 2018) and label proportion (LProp) learning (Quadrianto et al., 2008; Scott & Zhang, 2020; Zhang et al., 2022) as common examples. The weak supervision here usually denotes statistics over a group of instances. Pairwise observation, a special case of aggregate observation, deals with pairs of instances. Pairwise comparison (Pcomp) (Feng et al., 2021) and pairwise similarity (PSim) (Bao et al., 2018; Zhang et al., 2020), along with more recent developments such as similarity confidence (SimConf) (Cao et al., 2021b) and confidence difference (ConfDiff) (Wang et al., 2023a), fall into this category. Similarity, comparison, confidence scores, and relationships from the pre-trained models are usually adopted as weak supervision for pairwise observations. The fourth category, unlabeled data, is often supplemented by the labeled dataset as the weak supervision in this setting, which is sometimes complemented by the class's prior information. Semi-supervised learning (SemiSL) (Sohn et al., 2020; Xie et al., 2020; Zhang et al., 2021; Wang et al., 2023b; Chen et al., 2023), positive unlabeled (PosUlb) learning (du Plessis et al., 2015; Hammoudeh & Lowd, 2020; Chen et al., 2020; Garg et al., 2021; Kiryo et al., 2017; Zhao et al., 2022), similarity dissimilarity unlabeled (SDUlb) learning (Shimada et al., 2021), and Unlabeled unlabeled (UlbUlb) learning (Lu et al., 2018; Tang et al., 2023) fall into this category. Our framework is capable of addressing and unifying these diverse categories.

2.2. Towards the Unification of Weak Supervision

Although researchers have invested significant efforts in finding solutions to different forms of weak supervision, the practical unification of these problems still remains a distant goal. PosUlb, SDUlb, and UlbUlb learning can be connected to each other by substituting parameters (Lu et al., 2018; Feng et al., 2021). Zhang et al. (2020) have developed a probabilistic framework for pairwise (Hsu et al., 2019) and triplet comparison (Cui et al., 2020). Shukla et al. (2023) proposed a unified solution for weak supervision involving count statistics. They used a dynamic programming method over the aggregate observation to compute and maximize the count loss of $P(W|Y, X; \theta)$, corresponding to the supervised term in our EM formulation. The computational complexity is thus quadratic to the group length since the proposed dynamic programming algorithm iterates through the entire group. Wei et al. (2023) introduced the universal unbiased method (UUM) for aggregate observation, which is also interpretable from the EM perspective. Based on the assumptions of conditional independence of instances within a group and weak supervision given true labels, Wei et al. (2023) derived closed-form objectives for MultiIns, LProp, and PSim settings. However, the oversimplification of conditional independence limits UUM's scalability, particularly for LProp learning with long sequences. Chiang & Sugiyama (2023) provided a comprehensive risk analysis for various types of weak supervision from the perspective of the contamination matrix. Our framework offers a versatile and scalable solution, capable of efficiently handling a wider range of weak supervision without the limitations imposed by oversimplifications or computational complexity.

3. Method

In this section, we introduce our proposed framework and algorithm for learning from arbitrary weak supervision (GLWS). GLWS is based on the EM formulation (Dempster et al., 1977), where we consider the precise labels as the latent variable. We introduce an NFA (Rabin & Scott, 1959) modeling of weak supervision, which allows us to compute EM using the forward-backward algorithm in linear time.

3.1. Preliminaries

Let $\mathbf{x} \in \mathcal{X}$ be a training instance and $y \in \mathcal{Y}$ the corresponding precise supervision, where the input space $\mathcal{X} \subset \mathbb{R}^D$ has D dimensions, and the label space $\mathcal{Y} = [K-1] := \{0, 1, \ldots, K-1\}$ encompasses a total of K classes. In fully supervised learning, the training dataset with complete and precise annotations is defined as $\mathcal{D} = \{(\mathbf{x}_i, y_i)\}_{i \in [N]}$ and consists of N samples. Assume that each training example $(\mathbf{x}, y)$ is identically and independently sampled from the joint distribution $p(\mathbf{x}, y)$. The classifier $f(\theta) : \mathcal{X} \to \mathbb{R}^K$ predicts $p(y|\mathbf{x}; \theta)$ with learnable parameters θ, and is trained to maximize the log-likelihood $\log P(X, Y; \theta)$:

$$\theta^* = \arg\max_{\theta} \log P(X, Y; \theta). \tag{1}$$

This process results in the cross-entropy (CE) loss function:

$$\mathcal{L}_{\text{Full}} = \sum_{i=1}^{N} \sum_{k=0}^{K} -\mathbb{1}[y_i = k] \log p(y_i|\mathbf{x}_i; \theta). \tag{2}$$

3.2. General Framework for Weak Supervision

In practice, we may not have fully accessible precise supervision, i.e., Y is unknown. Instead, we may encounter various types of weak supervision for training instances, e.g., instance-wise label candidates, aggregated count statistics, pairwise similarity, unlabeled data, etc. We define weak supervision abstractly as W, representing an arbitrary form of information given to the training instances. For example, in PartialL (Feng et al., 2020c; Wang et al., 2022a; Wu et al., 2022), W is given as a set of label candidates for each instance $\mathcal{S} \subseteq \mathcal{Y}$. In MultiIns (Maron & Lozano-Pérez, 1997;

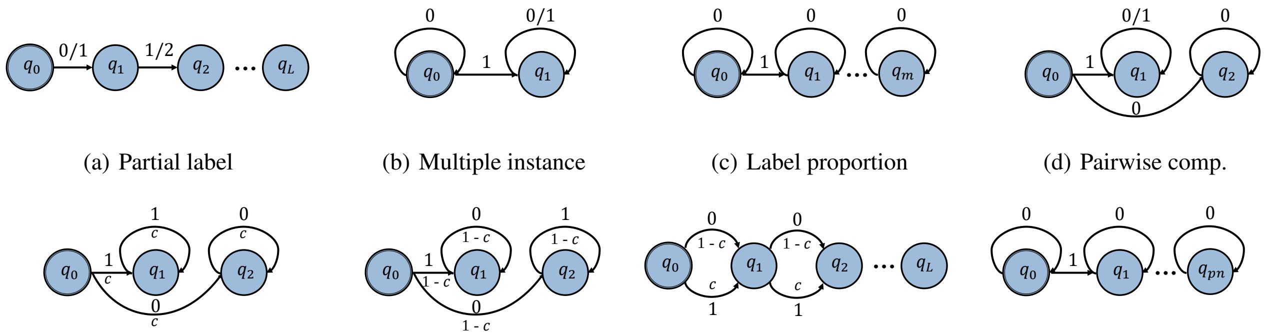

(a) Partial label (b) Multiple instance (c) Label proportion (d) Pairwise comp.

(e) Pairwise sim. (w/ conf. c) (f) Pairwise dissim. (w/ conf. c) (g) Positive conf. (w/ conf. c) (h) Unlabeled data (w/ prior p)

Figure 3. NFA for common weak supervision types for a sequence input of size L. (a) Partial labels, where the NFA has L transitions for each input with partial labels as symbols; (b) Multiple instances, whose NFA has 2 states, and can only transit to the accepting state via 1 to ensure at least one positive instance in the sequence; (c) Label proportion, whose NFA has $m+1$ states for m positive samples in the sequence; (d) Pairwise comparison, whose NFA has 3 states and covers $\{(1,1),(1,0),(0,0)\}$; (e) Pairwise similarity with confidence score c. The NFA also has 3 states and covers $\{(1,1),(0,0)\}$. If c is given as in similarity confidence and confidence difference, each edge is weighted by c; (f) Pairwise dissimilarity with confidence c for $\{(1,0),(0,1)\}$; (g) Positive confidence, whose NFA also has L transitions weighted by confidence c; (h) Unlabeled data with class prior p. The NFA is equivalent to expectation of label count as pn.

Zhou, 2004) and LProp learning (Yu et al., 2014) that deals with aggregate observations, W is given as the count statistics for each label $\{\sum_{j=1}^{L}\mathbb{1}[y^j=k]\geq 1 \mid \forall k\in\mathcal{Y}\}$ and $\{\sum_{j=1}^{L}\mathbb{1}[y^j=k] \mid \forall k\in\mathcal{Y}\}$ over a group of L instances $\{\mathbf{x}^j\}_{j\in[L]}$[2], respectively. When W represents the precise labels, it recovers fully supervised learning. With W, we must estimate the model to maximize the likelihood of the data X and the information W we have been provided:

$$\begin{aligned}\theta^* &= \arg\max_{\theta} \log P(X,W;\theta)\\ &= \arg\max_{\theta} \sum\nolimits_{Y} \log P(X,W,Y;\theta).\end{aligned} \tag{3}$$

As Y is unknown and the marginalization over Y requires θ, it is infeasible to solve Eq. (3) in a closed form, and instead typically needs the iterative hill-climbing solutions like EM algorithm. Thus, the maximum log-likelihood estimation in Eq. (3) can be solved by iteratively maximizing the variational lower bound of the log-likelihood $\log P(X,W,Y;\theta)$:

$$\theta^{t+1} = \arg\max_{\theta} \mathbb{E}_{Y|X,W;\theta^t}\left[\log P(X,W,Y;\theta)\right], \tag{4}$$

where θ^t denotes the t-th estimation of θ. $P(Y|X,W;\theta^t)$ represents a distribution on all possible labelings imposed by W with θ^t. The log-likelihood is then maximized on the expectation over the distribution of all possible labelings. The derivation of Eq. (4) is provided in Appendix A.1.

To derive the loss function for arbitrary weak supervision that includes instance-level and group-level W from Eq. (4), without loss of generality, we treat the realization of training instances X and the corresponding true precise labels Y all as sequence: $\mathbf{x}^{1:L}=\{\mathbf{x}^j\}_{j\in[L]}$ and $y^{1:L}=\{y^j\}_{j\in[L]}$ of size L and L could be 1. We also treat different types of weak supervision $w\in W$ as the information given for the input sequence. The sequence can be naturally formed from a batch of training samples, an aggregate observation, or a pairwise observation. Each instance in the dataset is thus generalized to $\mathbf{x}_i\to\mathbf{x}_i^{1:L}$ with $L\geq 1$. We make the following assumption, which almost always holds in reality:

Assumption 3.1. The sequence of predictions on precise labels $y^{1:L}$ is conditionally independent given the whole sequence of inputs $\mathbf{x}^{1:L}$, i.e., $p(y^{1:L}|\mathbf{x}^{1:L})=\prod_j^L p(y^j|\mathbf{x}^{1:L})$.

This notation allows us to deal with different weak supervision for both instance and group/bag data more flexibly.

Proposition 3.2. *For weakly supervised learning problems, the training objectives can be derived from Eq. (4) as:*

$$\begin{aligned}&\mathcal{L}_{\mathrm{Weak}} = \mathcal{L}_{\mathrm{U}} + \mathcal{L}_{\mathrm{S}},\\ &\mathcal{L}_{\mathrm{U}} = \sum_{i=1}^{N}\sum_{j=1}^{L} -p(y_i^j|\mathbf{x}_i^{1:L},w_i;\theta^t)\log p(y_i^j|\mathbf{x}_i^j;\theta),\\ &\mathcal{L}_{\mathrm{S}} = \sum_{i}^{N} -\log p(w_i|\mathbf{x}_i^{1:L},y_i^{1:L};\theta).\end{aligned} \tag{5}$$

The detailed derivation of Eq. (5) is shown in Appendix A.2. Eq. (5) consists of two parts: an unsupervised loss $\mathcal{L}_{\mathrm{U}}$ that encourages the instance-wise predictions from the classifier to align with the probability of this prediction given all possible labelings imposed by W, and a supervised loss $\mathcal{L}_{\mathrm{S}}$ that encourages the sequence predictions to fulfill W.

3.3. Weak Supervision as NFA

Although the proposed EM formulation can deal with various types of weak supervision flexibly, it is still computational intensive to calculate the probability $p(y^j|\mathbf{x}^{1:L},w;\theta)$

[2] We use $\mathbf{x}_i$ (y_i) to denote an instance/group in dataset of size N, and $\mathbf{x}^j$ (y^j) to denote an instance in the group $\{\mathbf{x}^j\}_{j\in[L]}$ of size L. Each $\mathbf{x}_i$ (y_i) in the dataset can denote a group with $L\geq 1$.

and $p(w|y^{1:L}, \mathbf{x}^{1:L}; \theta)$ for all possible labelings imposed by the given weak supervision. For example, in LProp learning where W is the label count over a group of L instances, the complexity of finding all possible labelings is of factorial $\mathcal{O}(L!)$. In most cases, the complexity is of exponential $\mathcal{O}(K^L)$ where K is the total number of classes. Moreover, while some recent methods towards unification can also be related to the proposed EM formulation (Shukla et al., 2023; Wei et al., 2023), they both involve a certain degree of simplification to approximate the complete EM formulation, which limits their scalability, as discussed in Section 2.2. Our method notably distinguishes from the prior arts in that we tackle weak supervision with the *complete* EM.

Here, we present a novel perspective to overcome the infeasibility of computing the complete EM. Under the sequential view, we treat the problem of assigning labels $\{y^j\}_{j\in[L]}$ to inputs $\{\mathbf{x}^j\}_{j\in[L]}$ as generating a sequence of symbols $y^{1:L}$ to $\mathbf{x}^{1:L}$ fulfilling W. For simplicity, we only consider binary classification problems here. In Section 3.5, we will show the generalization to multi-class classification problems. This process naturally fits the mechanism of the NFA (Rabin & Scott, 1959). We can thus model weak supervision W as an NFA that defines a set of finite states and transition rules, summarizing all possible labelings imposed by W.

Definition 3.3. (Rabin & Scott, 1959) A Non-deterministic Finite Automaton (NFA) is defined as a tuple (Q, Σ, δ, q_0, F), where Q is a finite set of states, Σ is a finite set of symbols, δ is a transition function $Q \times \Sigma \to P(Q)$, $q_0 \in Q$ is the initial state, and $F \subseteq Q$ is a set of accepting states.

We define the NFA of weak supervision W similarly, with states Q, initial state q_0, and accepting states F determined by W, symbols $\Sigma = \mathcal{Y} = \{0, 1\}$, and a transition function δ defining the possible transitions between states. We can now represent all possible labelings imposed by W as the language accepted by the NFA: $\{y^{1:L}|\delta(q_0, y^{1:L}) \in F\}$. The problem of finding all possible labelings is thereby converted to modeling the NFA of different types of weak supervision. We present the modeling of NFA for common forms of W in Fig. 3. For example, in MultiIns learning (Fig. 3(b)) with W denoting at least one positive sample within a group instance, its NFA contains 2 states $Q = \{q_0, q_1\}$. The initial state q_0 can only transit to the accepting state q_1 via symbol 1 to ensure W is satisfied. Once reaching q_1, transit via 0 and 1 are both allowed. For LProp with m positive labels (Fig. 3(c)), its NFA must transit via 1 for m times from q_0 to q_m to satisfy W, resulting in $m + 1$ states.

3.4. The Forward-Backward Algorithm

We are now set to compute the EM formulation with NFA.

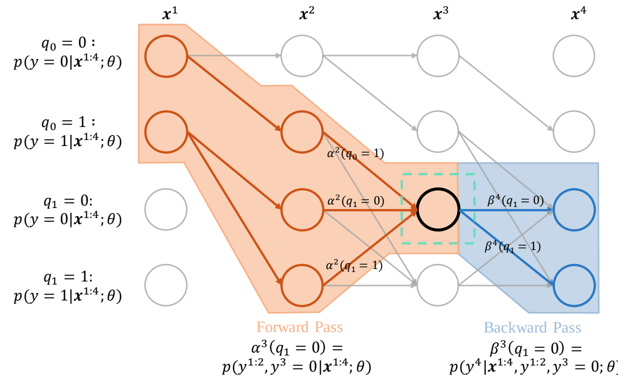

Figure 4. Illustration of the forward pass and backward pass in forward-backward algorithm to compute $p(y^j, w|\mathbf{x}^{1:L}; \theta^t)$.

Proposition 3.4. *Given the inputs $\mathbf{x}^{1:L}$, we treat the outputs sequence from the classifier $p(y^{1:L}|\mathbf{x}^{1:L}; \theta)$ as a linear chain graph. By taking the product on the linear chain graph of $p(y^{1:L}|\mathbf{x}^{1:L}; \theta)$ and the NFA graph of W, we obtain the trellis in the resulting graph as possible labelings.*

We have $p(y^j|\mathbf{x}^{1:L}, w; \theta^t) \propto p(y^j, w|\mathbf{x}^{1:L}; \theta^t)$ from Bayes' theorem, where the latter denotes the total probability of all valid labelings that go through y^j, and $p(w|y^{1:L}, \mathbf{x}^{1:L}; \theta)$ in Eq. (5) denotes the total probability from accepting states of the resulting graph. Fortunately, both the probability of $p(y^j, w|\mathbf{x}^{1:L}; \theta^t)$ and $p(w|y^{1:L}, \mathbf{x}^{1:L}; \theta)$ can be computed in linear time to the sequence length with dynamic programming on the trellis of the resulting graph, specifically the forward-backward algorithm (Rabiner, 1989; Graves et al., 2006). The core idea of the forward-backward algorithm is that the sum over paths corresponding to a labeling can be broken down into iterative sum over paths corresponding to the prefixes and the postfixes of that labeling. Thus, the probabilities can be obtained iteratively in linear time.

We illustrate the *trellis* expanded from the NFA of W in MultiIns learning with $L = 4$, with the help of Fig. 2 (more illustrations on other settings are shown in Appendix B.1), and the process of the forward-backward algorithm as shown in Fig. 4. The resulting graph has 4 states at each step of the sequence, where the first two correspond to q_0, the others to q_1, and the trellis to the transition rules in NFA. Each path from $\mathbf{x}^1$ to $\mathbf{x}^L$ denotes an available labeling. To compute the probabilities, we define the forward score $\alpha^j(q = y)$ and backward score $\beta^j(q = y)$ for each state q at step j:

$$\begin{aligned}
\alpha^j(q = y) &= \sum_{y' \in \{y^{i-1}|\delta(q_0, y^{1:L}) \in F\}} \alpha^{i-1}(q = y') p(y^j|\mathbf{x}^{1:L}; \theta^t), \\
\hat{\beta}^j(q = y) &= \sum_{y' \in \{y^{j+1}|\delta(q_0, y^{1:L}) \in F\}} \hat{\beta}^{j+1}(q = y') p(y^j|\mathbf{x}^{1:L}; \theta^t), \\
\beta^j(q = y) &= \frac{\hat{\beta}^j(q = y)}{p(y^j|\mathbf{x}^{1:L}; \theta^t)},
\end{aligned} \tag{6}$$

where $\hat{\beta}^j(q = y)$ is used as a proxy for easier computation of $\beta^j(q = y)$ (Graves et al., 2006). The forward score $\alpha^j(q = y)$ indicates the total probability of all preceding labeling that fulfills W at j-th inputs with

$p(y^{1:j}|\mathbf{x}^{1:L};\theta^t)$, and correspondingly, the backward score $\beta^j(q=y)$ indicates the total probability of all succeeding labeling that fulfills W at j-th inputs given the preceding $p(y^{j+1:L}|\mathbf{x}^{1:L}, y^{1:j};\theta^t)$, $\forall y^j \in \{y^j|\delta(q_0, y^{1:L}) \in F\}$. Both $\alpha^j(q=y)$ and $\beta^j(q=y)$ can be calculated recursively through the forward and backward pass on the graph, with *linear complexity of* $\mathcal{O}(|Q|L)$, where $|Q|$ is the number of states on the NFA of W. The joint probability at each position of the sequence thus can be calculated as:

$$p(y^j, w|\mathbf{x}^{1:L};\theta^t) = \textstyle\sum_{q\in Q} \frac{\alpha^j(q=y^j)\beta^j(q=y^j)}{\sum_{y'\in\mathcal{Y}}\alpha^j(q=y')\beta^j(q=y')}. \quad (7)$$

Moreover, the probability for supervised objective can also be easily computed as the summation of the probabilities at the accepting nodes on the graph with linear complexity:

$$p(w|y^{1:L}, \mathbf{x}^{1:L};\theta) = \sum_{q\in F}\sum_{y'\in\mathcal{Y}} \alpha^L(q=y'). \quad (8)$$

Now, we can bring these quantities back to Eq. (5) to perform training. In practice, we implement the forward-backward algorithm in log space and adopt the re-scaling strategy (McAuley & Leskovec, 2013) for numerical stability. We present the pseudo-algorithm of the forward-backward process of the common settings in Appendix B.2.

3.5. Extension to Multi-Class or Multi-Label Scenarios

In the analysis above, we model the NFA of W only for binary classification problems. Here, we demonstrate how to extend the modeling to multi-class (multi-label) classification problems. While it is natural to extend to multiple classes, for example, for partial labels as shown in Fig. 3(a), it is not straightforward to directly model the NFA of W with more than two values in its symbols Σ for aggregate observations. Considering the example with MultiIns learning, where the group of instances has two multi-class labels: at least one cat and at least one dog, the complexity of $|Q|$ in the NFA modeling will increase exponentially, thus also increasing the complexity in computing the loss functions. Instead, to deal with it, we treat each class as a separate positive class and other classes as a negative class, build an NFA on this class, and train each class as a binary classification problem with binary cross-entropy (BCE) loss. This is the common technique widely adopted in pre-training (Wightman et al.; Touvron et al., 2022) and we demonstrate its effectiveness in Section 4.2 for weakly supervised learning.

4. Experiments

In this section, we demonstrate the universality and effectiveness of the proposed method comprehensively on various weakly supervised learning settings. We conduct the evaluation mainly on CIFAR-10 (Krizhevsky et al., 2009), CIFAR-100 (Krizhevsky et al., 2009), STL-10 (Coates et al., 2011), and ImageNet-100 (Russakovsky et al., 2015). Results on MNIST (Deng, 2012) and F-MNIST (Xiao et al., 2017) are included in the Appendix, where most of the baseline methods were evaluated. We compare our method (GLWS) on 11 weak supervision settings of partial labels in Section 4.1, aggregate observations in Section 4.2, pairwise observations in Section 4.3, and unlabeled data in Section 4.4. Additionally, we provide more analysis and discussion in Section 4.5. We develop a codebase for implementations and experiments of all baselines and the proposed method, which will be open-sourced. Experiments are conducted three times with the average performance and standard deviation reported.

Table 1. Accuracy on partial label (PartialL) learning for instance-wise weak supervision. All results are averaged over three runs.

Dataset	CIFAR-10		CIFAR-100		STL-10		ImageNet-100	
Ratio	0.50	0.70	0.10	0.20	0.10	0.30	0.01	0.05
CC	92.51$\pm$0.04	89.01$\pm$0.20	77.44$\pm$0.32	74.60$\pm$0.17	77.02$\pm$0.69	73.26$\pm$0.34	73.14$\pm$0.94	64.67$\pm$0.74
LWS	85.66$\pm$0.32	80.71$\pm$0.10	50.67$\pm$0.33	43.51$\pm$0.32	67.65$\pm$0.33	58.18$\pm$1.65	72.04$\pm$0.77	62.13$\pm$0.95
PRODEN	93.32$\pm$0.23	90.26$\pm$0.20	77.50$\pm$0.15	74.89$\pm$0.13	77.44$\pm$0.26	73.19$\pm$1.05	78.61$\pm$0.63	77.59$\pm$0.60
PiCO	93.85$\pm$0.60	91.11$\pm$0.70	77.80$\pm$0.31	74.99$\pm$0.57	77.74$\pm$0.52	74.18$\pm$0.41	80.93$\pm$0.81	78.74$\pm$1.34
RCR	94.04$\pm$0.02	91.45$\pm$0.10	78.03$\pm$0.07	75.40$\pm$0.12	78.02$\pm$0.40	74.67$\pm$0.56	81.52$\pm$0.94	79.67$\pm$1.22
GLWS	**94.31**$\pm$0.09	**92.06**$\pm$0.14	**78.35**$\pm$0.11	**75.82**$\pm$0.25	**78.56**$\pm$0.27	**74.79**$\pm$0.21	**82.66**$\pm$0.54	**81.09**$\pm$0.50

4.1. Partial Labels

Setup. Here, we evaluate the proposed method of PartialL learning for multi-class classification, where W is a set of label candidates for each training instance. Following Wu et al. (2022) and Lv et al. (2020), we generate synthetic uniform partial labels for each dataset. We uniformly select labels other than the ground truth label with a specified partial ratio. For baselines, we adopt CC (Feng et al., 2020b), LWS (Wen et al., 2021), PRODEN (Lv et al., 2020), PiCO (Wang et al., 2022a), and RCR (Wu et al., 2022). We follow the hyper-parameters from Wu et al. (2022) for training all methods, with more details provided in Appendix C.2.1.

Results. The main results are shown in Table 1. Due to space limitations, more results are presented in Table 8 of Appendix C.2.2. Our method generally outperforms the baselines across different partial ratios, especially on the more practical ImageNet-100 with an improvement margin over RCR of **1.28%**. The complete EM formulation serves as a generalized method of the prior arts. Moreover, our method is simple and straightforward to implement, requiring no additional loss functions like the contrastive loss in PiCO or training tricks like multiple augmentations in RCR.

4.2. Aggregate Observations

Setup. For aggregate observations, we evaluate two common settings: MultiIns learning and LProp learning. MultiIns learning considers W as the indicator of at least one positive sample for a class in a bag of instances, while LProp learning views W as the exact count or proportion of positive samples for a class within the bag. We form training bags with instances sampled randomly, where the bag size is Gaussian-distributed with specified parameters. Previous

Table 2. Accuracy on multi-class multi-label aggregate observations of multiple instance (MultiIns) learning and label proportion (LProp) learning. All results are averaged over three runs.

Dataset	CIFAR-10		CIFAR-100		STL-10		ImageNet-100	
Dist	$\mathcal{N}(10,2)$	$\mathcal{N}(20,5)$	$\mathcal{N}(5,1)$	$\mathcal{N}(10,2)$	$\mathcal{N}(5,1)$	$\mathcal{N}(10,2)$	$\mathcal{N}(3,1)$	$\mathcal{N}(5,1)$
# Bags	5,000	2,500	10,000	5,000	2,000	1,000	20,000	20,000
Multiple Instance Learning								
Count Loss	86.84±0.34	65.97±0.94	52.04±1.49	30.66±0.68	73.79±1.51	63.80±1.66	71.48±1.61	70.58±1.14
UUM	13.86±1.31	13.21±0.52	1.27±0.29	1.01±0.20	18.25±2.58	15.45±1.66	1.33±0.17	1.25±0.18
GLWS	**87.15**±0.32	**71.88**±0.55	**56.28**±1.16	**52.29**±2.93	**74.66**±1.64	**64.35**±0.52	**73.92**±1.38	**73.08**±1.76
Label Proportion Learning								
LLP-VAT	85.33±0.44	79.70±0.48	51.95±2.74	52.26±0.46	74.76±0.08	70.76±0.78	59.97±3.45	68.45±1.82
Count Loss	89.46±0.24	84.54±0.39	54.13±1.43	36.21±0.49	76.60±0.13	73.36±0.33	72.17±0.47	72.21±0.91
UUM	-	-	53.25±1.96	-	77.26±0.67	-	71.51±0.94	71.14±1.31
GLWS	**89.77**±0.45	**86.41**±0.11	**58.25**±0.61	**57.14**±1.71	**78.27**±0.77	**73.70**±0.19	**73.93**±0.33	**73.09**±0.84

methods typically focus on binary classification in these settings. However, in our main paper, we extend this to multi-class classification (additional binary classification results are in Appendix C.3.2), with W being multi-labeled. For instance, in MultiIns learning, the weak supervision could indicate that at least one positive instance for both dog and cat classes are present in a group. Baselines for our evaluation include Count Loss (Shukla et al., 2023) and UUM (Wei et al., 2023). In LProp learning, we also compare against LLP-VAT (Tsai & Lin, 2020). Details of training hyper-parameters are shown in Appendix C.3.1.

Results. The results are presented in Table 2. Our method demonstrates a significant performance gain compared to baselines across various setups. In MultiIns learning, our method surpasses Count Loss by **1.46**% on CIFAR-10, **12.93**% on CIFAR-100, 0.71% on STL-10, and **2.47**% on ImageNet-100, showcasing its effectiveness in more complex datasets with a larger number of classes and training group sizes. For LProp learning, it notably outperforms previous methods, with improvements of **4.50**% on CIFAR-100 and **2.19**% on ImageNet-100. The oversimplified modeling of UUM, while adequate for smaller bags and datasets (e.g., sizes 3 and 5, MNIST and Fashion-MNIST as shown in Table 10), makes it struggle with larger datasets and bag sizes as shown in Table 2. Furthermore, for bags with an average size greater than 5, LProp learning becomes computationally infeasible in UUM due to the factorial complexity. Compared to UUM's factorial complexity and Count Loss's quadratic complexity, our proposed method efficiently addresses various settings with linear complexity.

4.3. Pairwise Observations

Setup. We conduct evaluation on four common settings of pairwise observations $(\mathbf{x}^1, \mathbf{x}^2)$ for binary classification: PComp (Feng et al., 2021), PSim (Wei et al., 2023), SimConf (Cao et al., 2021b), and ConfDiff learning (Wang et al., 2023a). We treat a subset of classes of each dataset as the positive class, and others as the negative class. Details on the class split are shown in Appendix C.1. We first set a class prior, and then sample data to form the training pairs accordingly for each setting, following the baselines (Feng et al., 2021; Wei et al., 2023; Cao et al., 2021b; Wang et al., 2023a). For PComp, W indicates the unlabeled pairs that $\mathbf{x}^1$ can only be more positive than $\mathbf{x}^2$. We adopt PComp (and its variants) (Feng et al., 2021) and Rank Pruning (Northcutt et al., 2017) as baselines. For PSim, W indicates whether the instances in the pair have similar labels or dissimilar labels. We use RiskSD (Shimada et al., 2021) and UUM (Wei et al., 2023) as baselines for this setting. For SimConf and ConfDiff, W is the confidence score of similarity and difference between $\mathbf{x}^1$ and $\mathbf{x}^2$, respectively. The confidence score is given by a pre-trained model, and we follow the previous method (Cao et al., 2021b; Wang et al., 2023a) to train a model on excluded data first to compute the confidence score. We additionally adopt CLIP (Radford et al., 2021; Cherti et al., 2023) with its zero-shot confidence score. Since only a non-identifiable classifiers can be learned from pairwise observations, we use clustering algorithms of Hungarian matching (Crouse, 2016) similar to Wei et al. (2023) on the predictions to evaluate. We present more training details of these settings in Appendix C.4.1.

Table 3. Accuracy on binary classification of pairwise comparison (PComp) and pairwise similarity (PSim) averaged over three runs.

Dataset	CIFAR-10		CIFAR-100		STL-10	
Pairwise Comparison						
#Pairs	20,000		20.000		5,000	
Prior	0.5	0.8	0.5	0.8	0.5	0.8
PComp ABS	91.78±0.10	87.37±1.89	81.67±0.24	66.06±1.19	79.07±0.40	56.45±1.86
PComp ReLU	92.18±0.22	90.57±0.21	81.77±0.59	66.57±1.27	79.68±0.75	67.01±1.71
PComp Teacher	93.33±0.38	91.35±0.27	78.59±0.60	67.43±3.09	77.33±0.14	72.88±0.15
PComp Unbiased	91.71±0.48	88.22±0.58	67.80±0.07	60.86±2.19	77.46±0.19	71.60±0.95
Rank Pruning	93.98±0.40	91.97±0.27	78.90±0.48	71.51±0.73	77.89±0.42	73.62±1.38
GLWS	**94.15**±0.10	**93.28**±0.38	**83.15**±0.16	**80.50**±0.20	**81.26**±0.54	**79.24**±0.87
Pairwise Similarity						
#Pairs	25,000		25.000		5,000	
Prior	0.4	0.6	0.4	0.6	0.4	0.6
RiskSD	85.78±1.70	85.61±1.34	70.41±0.21	64.26±3.81	74.15±3.27	69.35±0.32
UUM	97.24±0.23	97.16±0.24	87.13±0.40	85.19±2.45	83.55±0.80	83.64±0.25
GLWS	**97.44**±0.07	**97.18**±0.22	**87.25**±0.16	**86.96**±0.33	**84.81**±0.60	**85.19**±0.26

Table 4. Accuracy on binary classification of similarity confidence (SimConf) and confidence difference (ConfDiff) over three runs.

Dataset	CIFAR-10		CIFAR-100		STL-10	
#Pairs	25,000		25.000		5,000	
Prior	0.4	0.4	0.4	0.4	0.4	0.4
Conf Model	WRN-28-2	CLIP ViT-B-16	ResNet-18	CLIP ViT-B-16	ResNet-18	CLIP ViT-B-16
Similarity Confidence						
Sconf Abs	87.36±1.22	90.16±1.32	75.79±0.27	69.51±0.44	76.84±0.75	74.44±0.78
Sconf ReLU	88.56±0.57	90.50±0.44	74.95±0.55	69.67±1.51	77.40±0.31	75.26±0.66
Sconf NN Abs	89.04±0.88	89.05±2.11	74.55±0.23	68.93±2.00	77.55±0.31	75.66±0.51
Sconf Unbiased	88.72±0.52	88.71±0.59	72.87±1.30	69.55±0.31	77.76±0.40	74.36±0.60
GLWS	**95.97**±0.11	**97.88**±0.11	**85.58**±0.88	**87.94**±0.34	**78.64**±0.16	**79.06**±0.05
Confidence Difference						
ConfDiff Abs	90.12±4.19	88.61±7.50	82.89±0.32	81.45±0.26	73.17±2.06	77.33±0.74
ConfDiff ReLU	90.36±4.07	88.78±7.91	83.13±0.27	81.68±0.46	72.39±3.06	77.59±0.17
ConfDiff Unbiased	90.05±5.23	87.91±9.03	83.65±0.11	81.94±0.43	72.13±2.70	77.98±0.08
GLWS	**95.36**±0.19	**96.14**±0.67	**86.12**±0.76	**83.42**±1.12	**77.99**±0.75	**78.49**±0.31

Results. We present the main results for PComp and Psim in Table 3, and for SimConf and ConfDiff in Table 4. The proposed method presents consistent and superior performance, where the improvement margin is significant especially on larger datasets. On CIFAR-100, our method improves the previous best by **10.23**% on pairwise comparison and by **14.03**% on similarity confidence. All the baseline methods

Table 5. Accuracy on positive unlabeled (PosUlb) learning for binary classification. All results are averaged over three runs.

	CIFAR-10		CIFAR-100		STL-10	
# Pos	500	1000	1000	2000	500	1000
Count Loss	87.76±0.59	88.61±0.68	70.57±1.50	78.13±0.19	77.11±0.60	78.79±0.96
CVIR	88.65±2.59	93.37±0.24	78.56±0.22	82.94±0.37	77.67±1.11	81.84±1.10
Dist PU	83.61±4.52	82.60±2.48	69.12±1.39	69.83±1.43	71.07±1.12	70.89±0.63
NN PU	87.45±0.66	90.32±0.50	75.49±0.88	77.26±0.47	74.57±0.54	77.32±0.95
U PU	81.38±2.17	87.51±0.24	68.70±0.79	70.08±0.98	73.37±0.57	75.31±0.74
Var PU	77.00±2.82	84.45±2.58	61.02±0.22	66.02±0.29	60.98±0.78	62.37±1.44
GLWS	**91.67**±0.19	**93.69**±0.28	**80.30**±0.12	**83.32**±0.23	**79.60**±0.95	**82.87**±0.83

here require the class prior in the proposed loss functions, which must be given or estimated. Ours does not require class prior and still achieves the best performance. More results of pairwise observations are in Appendix C.4.2.

4.4. Unlabeled Data

Setup. For unlabeled data, we consider the settings of binary classification where only the class prior is given to the unlabeled data as weak supervision: PosUlb (du Plessis et al., 2015), UlbUlb (Lu et al., 2018), and SDUlb learning (Shimada et al., 2021). We present only the results of PosUlb learning in the main paper, and other settings are shown in Appendix C.5.2. We similarly split the classes into either the positive subset or the negative subset as pairwise observations. For PosUlb learning, we first randomly select a specified number of positive samples as a labeled set, and treat the remaining data as an unlabeled set. For STL-10, we additionally add its split of extra data to the unlabeled set. We consider Count Loss (Shukla et al., 2023), CVIR (Garg et al., 2021), DistPU (Zhao et al., 2022), NNPU (Kiryo et al., 2017), UPU (Kiryo et al., 2017), and VarPU (Chen et al., 2020) as baselines. More details are in Appendix C.5.1.

Results. On weak supervision with unlabeled data, our method also presents superior performance, as shown in Table 5. Notably, our method outperforms the previous best by **3.02**% on CIFAR-10 with 500 positive labeled data and **4.81**% on CIFAR-100 with 1000 positive labeled data. Compared to Count Loss, which computes only the supervised objective in the proposed EM formulation with quadratic complexity, its performance often falls short of other baselines such as CVIR. Our method only requires linear time.

4.5. Analysis and Discussion

Convergence. EM algorithm might be notoriously known for difficulty in convergence and converging to local minima. We present the convergence plots, especially for aggregate observations with long sequence lengths, to show that this is not a limitation for GLWS in weakly supervised learning. As shown in Fig. 5, our method converges faster to a better solution with a more stable training process (narrower error bars), compared to Count Loss (Shukla et al., 2023).

Runtime. We compare the running time explicitly in Fig. 6

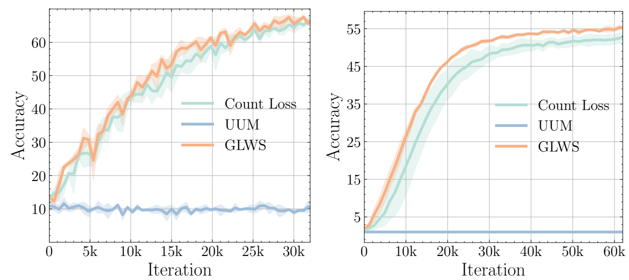

(a) CIFAR-10, $\mathcal{N}(20, 5)$ (b) CIFAR-100, $\mathcal{N}(10, 2)$

Figure 5. Convergence of accuracy with error bar on multiple instance learning with long input sequence. (a) CIFAR-10 with bag length distribution of $\mathcal{N}(20, 5)$; (b) CIFAR-100 with $\mathcal{N}(10, 2)$. Our method shows superior convergence with more stable training.

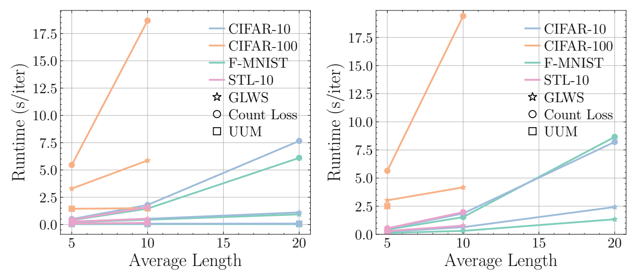

(a) Multiple instance (b) Label proportion

Figure 6. Runtime (s/iter.) vs. average input length for aggregate observations on evaluated datasets. (a) Multiple instance; (b) Label proportion. Our method shows a reasonable runtime trade-off.

for aggregate observations. It is obvious that Count Loss (Shukla et al., 2023) presents (approximately) a quadratic trend in runtime as input length increases. UUM (Wei et al., 2023) shows consistent runtime for MultiIns learning with its oversimplification, leading to a practical performance gap as shown in Table 2 and Table 10. On label proportion, it is only applicable to input length of 5 because of its factorial complexity. Ours achieves the most reasonable performance and runtime trade-off with the proposed efficient algorithm.

Extension. Our framework is flexibly extensible to other settings (shown in Appendix C.6) and also adaptable to noisy weak supervision $\hat{W}$ with an inherent learnable noise model $P(W|\hat{W};\theta)$ in the EM, which is left for future work.

5. Conclusion

In this paper, we demonstrated a general framework for learning from arbitrary weak supervision that unifies various forms of weak supervision and can be extended to more settings flexibly, including instance partial labels, aggregate observations, pairwise observations, and unlabeled data, which addresses a significant gap in the practical applicability and scalability of weakly supervised learning methods. Experiments across various settings and practical datasets validated the superiority of the proposed method. We hope our work can inspire more research on weak supervision.

Impact Statement

This paper presents work whose goal is to advance the field of Machine Learning. There are many potential societal consequences of our work, none of which we feel must be specifically highlighted here.

References

Bao, H., Niu, G., and Sugiyama, M. Classification from pairwise similarity and unlabeled data. In *International Conference on Machine Learning*, pp. 452–461. PMLR, 2018.

Bao, H., Shimada, T., Xu, L., Sato, I., and Sugiyama, M. Pairwise supervision can provably elicit a decision boundary. *arXiv preprint arXiv:2006.06207*, 2020.

Cao, Y., Feng, L., Shu, S., Xu, Y., An, B., Niu, G., and Sugiyama, M. Multi-class classification from single-class data with confidences. *arXiv preprint arXiv:2106.08864*, 2021a.

Cao, Y., Feng, L., Xu, Y., An, B., Niu, G., and Sugiyama, M. Learning from similarity-confidence data. In *International Conference on Machine Learning*, pp. 1272–1282. PMLR, 2021b.

Chen, H., Liu, F., Wang, Y., Zhao, L., and Wu, H. A variational approach for learning from positive and unlabeled data. *Advances in Neural Information Processing Systems*, 33:14844–14854, 2020.

Chen, H., Tao, R., Fan, Y., Wang, Y., Wang, J., Schiele, B., Xie, X., Raj, B., and Savvides, M. Softmatch: Addressing the quantity-quality trade-off in semi-supervised learning. In *International Conference on Learning Representations (ICLR)*, 2023.

Cherti, M., Beaumont, R., Wightman, R., Wortsman, M., Ilharco, G., Gordon, C., Schuhmann, C., Schmidt, L., and Jitsev, J. Reproducible scaling laws for contrastive language-image learning. In *Proceedings of the IEEE/CVF Conference on Computer Vision and Pattern Recognition*, pp. 2818–2829, 2023.

Chiang, C.-K. and Sugiyama, M. Unified risk analysis for weakly supervised learning. *arXiv preprint arXiv:2309.08216*, 2023.

Coates, A., Ng, A., and Lee, H. An analysis of single-layer networks in unsupervised feature learning. In *Proceedings of the fourteenth international conference on artificial intelligence and statistics*, pp. 215–223. JMLR Workshop and Conference Proceedings, 2011.

Cour, T., Sapp, B., and Taskar, B. Learning from partial labels. *The Journal of Machine Learning Research*, 12: 1501–1536, 2011.

Crouse, D. F. On implementing 2d rectangular assignment algorithms. *IEEE Transactions on Aerospace and Electronic Systems*, 52(4):1679–1696, 2016.

Cui, Z., Charoenphakdee, N., Sato, I., and Sugiyama, M. Classification from triplet comparison data. *Neural Computation*, 32(3):659–681, 2020.

Dehghani, M., Djolonga, J., Mustafa, B., Padlewski, P., Heek, J., Gilmer, J., Steiner, A. P., Caron, M., Geirhos, R., Alabdulmohsin, I., et al. Scaling vision transformers to 22 billion parameters. In *International Conference on Machine Learning*, pp. 7480–7512. PMLR, 2023.

Dempster, A. P., Laird, N. M., and Rubin, D. B. Maximum likelihood from incomplete data via the em algorithm. *Journal of the royal statistical society: series B (methodological)*, 39(1):1–22, 1977.

Deng, L. The mnist database of handwritten digit images for machine learning research. *IEEE Signal Processing Magazine*, 29(6):141–142, 2012.

Denœux, T. Maximum likelihood estimation from fuzzy data using the em algorithm. *Fuzzy sets and systems*, 183 (1):72–91, 2011.

du Plessis, M., Niu, G., and Sugiyama, M. Convex formulation for learning from positive and unlabeled data. In *International conference on machine learning*, pp. 1386–1394. PMLR, 2015.

Feng, L., Kaneko, T., Han, B., Niu, G., An, B., and Sugiyama, M. Learning with multiple complementary labels. In *Proceedings of the International Conference on Machine Learning (ICML)*, pp. 3072–3081. PMLR, 2020a.

Feng, L., Lv, J., Han, B., Xu, M., Niu, G., Geng, X., An, B., and Sugiyama, M. Provably consistent partial-label learning. *ArXiv*, abs/2007.08929, 2020b.

Feng, L., Lv, J., Han, B., Xu, M., Niu, G., Geng, X., An, B., and Sugiyama, M. Provably consistent partial-label learning. *Advances in neural information processing systems*, 33:10948–10960, 2020c.

Feng, L., Shu, S., Lu, N., Han, B., Xu, M., Niu, G., An, B., and Sugiyama, M. Pointwise binary classification with pairwise confidence comparisons. In *International Conference on Machine Learning*, pp. 3252–3262. PMLR, 2021.

Gadre, S. Y., Ilharco, G., Fang, A., Hayase, J., Smyrnis, G., Nguyen, T., Marten, R., Wortsman, M., Ghosh, D., Zhang, J., et al. Datacomp: In search of the next generation of multimodal datasets. *arXiv preprint arXiv:2304.14108*, 2023.

Garg, S., Wu, Y., Smola, A., Balakrishnan, S., and Lipton, Z. C. Mixture proportion estimation and pu learning: A modern approach, 2021.

Graves, A., Fernández, S., Gomez, F., and Schmidhuber, J. Connectionist temporal classification: labelling unsegmented sequence data with recurrent neural networks. In *Proceedings of the International Conference on Machine Learning (ICML)*, pp. 369–376, 2006.

Hammoudeh, Z. and Lowd, D. Learning from positive and unlabeled data with arbitrary positive shift. *Advances in Neural Information Processing Systems*, 33:13088–13099, 2020.

He, K., Zhang, X., Ren, S., and Sun, J. Deep residual learning for image recognition. In *Proceedings of the IEEE/CVF Conference on Computer Vision and Pattern Recognition (CVPR)*, pp. 770–778, 2016.

Hsu, Y.-C., Lv, Z., Schlosser, J., Odom, P., and Kira, Z. Multi-class classification without multi-class labels. *arXiv preprint arXiv:1901.00544*, 2019.

Ilse, M., Tomczak, J., and Welling, M. Attention-based deep multiple instance learning. In *International Conference on Machine Learning (ICML)*, pp. 2127–2136. PMLR, 2018.

Ishida, T., Niu, G., and Sugiyama, M. Binary classification from positive-confidence data. *Advances in neural information processing systems*, 31, 2018.

Ishida, T., Niu, G., Menon, A., and Sugiyama, M. Complementary-label learning for arbitrary losses and models. In *International Conference on Machine Learning*, pp. 2971–2980. PMLR, 2019.

Ishida, T., Yamane, I., Charoenphakdee, N., Niu, G., and Sugiyama, M. Is the performance of my deep network too good to be true? a direct approach to estimating the bayes error in binary classification. *arXiv preprint arXiv:2202.00395*, 2022.

Kingma, D. P. and Ba, J. Adam: A method for stochastic optimization. *arXiv preprint arXiv:1412.6980*, 2014.

Kiryo, R., Niu, G., Du Plessis, M. C., and Sugiyama, M. Positive-unlabeled learning with non-negative risk estimator. *Advances in neural information processing systems*, 30, 2017.

Krizhevsky, A. et al. Learning multiple layers of features from tiny images. 2009.

Kück, H. and de Freitas, N. Learning about individuals from group statistics. In *Proceedings of the Twenty-First Conference on Uncertainty in Artificial Intelligence*, UAI'05, pp. 332–339, Arlington, Virginia, USA, 2005. AUAI Press. ISBN 0974903914.

LeCun, Y., Bottou, L., Bengio, Y., and Haffner, P. Gradient-based learning applied to document recognition. *Proceedings of the IEEE*, 86(11):2278–2324, 1998.

Loshchilov, I. and Hutter, F. Sgdr: Stochastic gradient descent with warm restarts. *International Conference on Learning Representations (ICLR)*, 2016.

Lu, N., Niu, G., Menon, A. K., and Sugiyama, M. On the minimal supervision for training any binary classifier from only unlabeled data. *arXiv preprint arXiv:1808.10585*, 2018.

Luo, J. and Orabona, F. Learning from candidate labeling sets. *Advances in Neural Information Processing Systems (NeurIPS)*, 2010.

Lv, J., Xu, M., Feng, L., Niu, G., Geng, X., and Sugiyama, M. Progressive identification of true labels for partial-label learning. In *Proceedings of the International Conference on Machine Learning (ICML)*, pp. 6500–6510. PMLR, 2020.

Maron, O. and Lozano-Pérez, T. A framework for multiple-instance learning. *Advances in Neural Information Processing Systems (NeurIPS)*, 10, 1997.

McAuley, J. and Leskovec, J. Hidden factors and hidden topics: understanding rating dimensions with review text. In *Proceedings of the 7th ACM conference on Recommender systems*, pp. 165–172, 2013.

Mireshghallah, F., Taram, M., Vepakomma, P., Singh, A., Raskar, R., and Esmaeilzadeh, H. Privacy in deep learning: A survey. *arXiv preprint arXiv:2004.12254*, 2020.

Northcutt, C. G., Wu, T., and Chuang, I. L. Learning with confident examples: Rank pruning for robust classification with noisy labels. *arXiv preprint arXiv:1705.01936*, 2017.

OpenAI. Gpt-4 technical report. 2023.

Pagano, T. P., Loureiro, R. B., Lisboa, F. V., Peixoto, R. M., Guimarães, G. A., Cruz, G. O., Araujo, M. M., Santos, L. L., Cruz, M. A., Oliveira, E. L., et al. Bias and unfairness in machine learning models: a systematic review on datasets, tools, fairness metrics, and identification and mitigation methods. *Big data and cognitive computing*, 7 (1):15, 2023.

Quadrianto, N., Smola, A. J., Caetano, T. S., and Le, Q. V. Estimating labels from label proportions. In *Proceedings of the 25th International Conference on Machine learning*, pp. 776–783, 2008.

Quost, B. and Denoeux, T. Clustering and classification of fuzzy data using the fuzzy em algorithm. *Fuzzy Sets and Systems*, 286:134–156, 2016.

Rabin, M. O. and Scott, D. Finite automata and their decision problems. *IBM journal of research and development*, 3(2):114–125, 1959.

Rabiner, L. R. A tutorial on hidden markov models and selected applications in speech recognition. *Proceedings of the IEEE*, 77(2):257–286, 1989.

Radford, A., Kim, J. W., Hallacy, C., Ramesh, A., Goh, G., Agarwal, S., Sastry, G., Askell, A., Mishkin, P., Clark, J., et al. Learning transferable visual models from natural language supervision. In *Proceedings of the International Conference on Machine Learning (ICML)*, pp. 8748–8763. PMLR, 2021.

Rombach, R., Blattmann, A., Lorenz, D., Esser, P., and Ommer, B. High-resolution image synthesis with latent diffusion models. In *Proceedings of the IEEE/CVF conference on computer vision and pattern recognition*, pp. 10684–10695, 2022.

Russakovsky, O., Deng, J., Su, H., Krause, J., Satheesh, S., Ma, S., Huang, Z., Karpathy, A., Khosla, A., Bernstein, M., et al. Imagenet large scale visual recognition challenge. *International journal of computer vision*, 115: 211–252, 2015.

Scott, C. and Zhang, J. Learning from label proportions: A mutual contamination framework. *Advances in Neural Information Processing Systems (NeurIPS)*, 33:22256–22267, 2020.

Settles, B., Craven, M., and Friedland, L. Active learning with real annotation costs. In *Proceedings of the NIPS workshop on cost-sensitive learning*, volume 1. Vancouver, CA:, 2008.

Shimada, T., Bao, H., Sato, I., and Sugiyama, M. Classification from pairwise similarities/dissimilarities and unlabeled data via empirical risk minimization. *Neural Computation*, 33(5):1234–1268, 2021.

Shukla, V., Zeng, Z., Ahmed, K., and Van den Broeck, G. A unified approach to count-based weakly-supervised learning. In *ICML 2023 Workshop on Differentiable Almost Everything: Differentiable Relaxations, Algorithms, Operators, and Simulators*, jul 2023. URL http://starai.cs.ucla.edu/papers/ShuklaDAE23.pdf.

Sohn, K., Berthelot, D., Carlini, N., Zhang, Z., Zhang, H., Raffel, C. A., Cubuk, E. D., Kurakin, A., and Li, C.-L. Fixmatch: Simplifying semi-supervised learning with consistency and confidence. *Advances in Neural Information Processing Systems (NeurIPS)*, 33, 2020.

Strobel, M. and Shokri, R. Data privacy and trustworthy machine learning. *IEEE Security & Privacy*, 20(5):44–49, 2022.

Sugiyama, M., Bao, H., Ishida, T., Lu, N., Sakai, T., and Niu, G. *Machine Learning from Weak Supervision: An Empirical Risk Minimization Approach*. MIT Press, Cambridge, Massachusetts, USA, 2022.

Tang, Y., Lu, N., Zhang, T., and Sugiyama, M. Multi-class classification from multiple unlabeled datasets with partial risk regularization. In *Asian Conference on Machine Learning*, pp. 990–1005. PMLR, 2023.

Tommasi, T., Patricia, N., Caputo, B., and Tuytelaars, T. A deeper look at dataset bias. *Domain adaptation in computer vision applications*, pp. 37–55, 2017.

Touvron, H., Cord, M., and Jégou, H. Deit iii: Revenge of the vit. In *European Conference on Computer Vision*, pp. 516–533. Springer, 2022.

Tsai, K.-H. and Lin, H.-T. Learning from label proportions with consistency regularization. In *Asian Conference on Machine Learning*, pp. 513–528. PMLR, 2020.

Van Rooyen, B. and Williamson, R. C. A theory of learning with corrupted labels. *Journal of Machine Learning Research*, 18(228):1–50, 2018.

Wang, D., Zhang, M.-L., and Li, L. Adaptive graph guided disambiguation for partial label learning. *IEEE Transactions on Pattern Analysis and Machine Intelligence*, 44: 8796–8811, 2019.

Wang, H., Xiao, R., Li, Y., Feng, L., Niu, G., Chen, G., and Zhao, J. PiCO: Contrastive label disambiguation for partial label learning. In *International Conference on Learning Representations (ICLR)*, 2022a. URL https://openreview.net/forum?id=EhYjZy6e1gJ.

Wang, W., Feng, L., Jiang, Y., Niu, G., Zhang, M.-L., and Sugiyama, M. Binary classification with confidence difference. *arXiv preprint arXiv:2310.05632*, 2023a.

Wang, Y., Chen, H., Fan, Y., Sun, W., Tao, R., Hou, W., Wang, R., Yang, L., Zhou, Z., Guo, L.-Z., Qi, H., Wu, Z., Li, Y.-F., Nakamura, S., Ye, W., Savvides, M., Raj, B., Shinozaki, T., Schiele, B., Wang, J., Xie, X., and Zhang, Y. Usb: A unified semi-supervised learning benchmark. In *Advances in Neural Information Processing Systems (NeurIPS)*, 2022b.

Wang, Y., Chen, H., Heng, Q., Hou, W., Fan, Y., , Wu, Z., Wang, J., Savvides, M., Shinozaki, T., Raj, B., Schiele, B., and Xie, X. Freematch: Self-adaptive thresholding for semi-supervised learning. In *International Conference on Learning Representations (ICLR)*, 2023b.

Wei, Z., Feng, L., Han, B., Liu, T., Niu, G., Zhu, X., and Shen, H. T. A universal unbiased method for classification from aggregate observations. In Krause, A., Brunskill, E., Cho, K., Engelhardt, B., Sabato, S., and Scarlett, J. (eds.), *Proceedings of the 40th International Conference on Machine Learning*, volume 202 of *Proceedings of Machine Learning Research*, pp. 36804–36820. PMLR, 23–29 Jul 2023. URL https://proceedings.mlr.press/v202/wei23a.html.

Wen, H., Cui, J., Hang, H., Liu, J., Wang, Y., and Lin, Z. Leveraged weighted loss for partial label learning. In *Proceedings of the International Conference on Machine Learning (ICML)*, pp. 11091–11100. PMLR, 2021.

Wightman, R., Touvron, H., and Jégou, H. Resnet strikes back: An improved training procedure in timm. arxiv 2021. *arXiv preprint arXiv:2110.00476*.

Wu, D.-D., Wang, D.-B., and Zhang, M.-L. Revisiting consistency regularization for deep partial label learning. In Chaudhuri, K., Jegelka, S., Song, L., Szepesvari, C., Niu, G., and Sabato, S. (eds.), *Proceedings of the International Conference on Machine Learning (ICML)*, volume 162 of *Proceedings of Machine Learning Research*, pp. 24212–24225. PMLR, 17–23 Jul 2022. URL https://proceedings.mlr.press/v162/wu22l.html.

Xiao, H., Rasul, K., and Vollgraf, R. Fashion-mnist: a novel image dataset for benchmarking machine learning algorithms, 2017.

Xie, Q., Dai, Z., Hovy, E., Luong, T., and Le, Q. Unsupervised data augmentation for consistency training. *Advances in Neural Information Processing Systems (NeurIPS)*, 33, 2020.

Yan, Y., Wang, X., Guo, X., Fang, J., Liu, W., and Huang, J. Deep multi-instance learning with dynamic pooling. In *Asian Conference on Machine Learning*, pp. 662–677. PMLR, 2018.

Yang, M., Zhang, Y.-X., Ye, M., and Min, F. Attention-to-embedding framework for multi-instance learning. In *Pacific-Asia Conference on Knowledge Discovery and Data Mining*, pp. 109–121. Springer, 2022.

Yu, F. X., Choromanski, K., Kumar, S., Jebara, T., and Chang, S.-F. On learning from label proportions. *arXiv preprint arXiv:1402.5902*, 2014.

Zagoruyko, S. and Komodakis, N. Wide residual networks. In *British Machine Vision Conference (BMVC)*. British Machine Vision Association, 2016.

Zhang, B., Wang, Y., Hou, W., Wu, H., Wang, J., Okumura, M., and Shinozaki, T. Flexmatch: Boosting semi-supervised learning with curriculum pseudo labeling. *Advances in Neural Information Processing Systems (NeurIPS)*, 34, 2021.

Zhang, J., Wang, Y., and Scott, C. Learning from label proportions by learning with label noise. *Advances in Neural Information Processing Systems*, 35:26933–26942, 2022.

Zhang, Y., Charoenphakdee, N., Wu, Z., and Sugiyama, M. Learning from aggregate observations. pp. 7993–8005, 2020.

Zhao, Y., Xu, Q., Jiang, Y., Wen, P., and Huang, Q. Dist-pu: Positive-unlabeled learning from a label distribution perspective. In *Proceedings of the IEEE/CVF Conference on Computer Vision and Pattern Recognition*, pp. 14461–14470, 2022.

Zhou, Z.-H. Multi-instance learning: A survey. *Department of Computer Science & Technology, Nanjing University, Tech. Rep*, 1, 2004.

Zhou, Z.-H. A brief introduction to weakly supervised learning. *National science review*, 5(1):44–53, 2018.

A. Proofs

A.1. Derivation of Eq. (4)

Evidence lower bound (ELBO), or equivalently variational lower bound (Dempster et al., 1977), is the core quantity in EM. We provide the detailed derivation for Eq. (4) here. To model $\log P(X, W; \theta)$:

$$\begin{aligned}
\log P(X, W; \theta) &= \log \sum_{Y} P(X, W, Y; \theta) \\
&= \log Q(Y) \frac{P(X, W, Y; \theta)}{Q(Y)} \\
&= \log \mathbb{E}_{Q(Y)}[\frac{P(X, W, Y; \theta)}{Q(Y)}] \\
&\geq \mathbb{E}_{Q(Y)}[\log \frac{P(X, W, Y; \theta)}{Q(Y)}] \quad \text{Jensen's inequality} \\
&= \mathbb{E}_{Q(Y)}[\log P(X, W, Y; \theta)] - \mathbb{E}_{Q(Y)}[\log Q(Y)] \\
&= ELBO(\theta, Q(Y)),
\end{aligned} \tag{9}$$

where the first term in ELBO is the lower bound and the second term is the entropy over $Q(Y)$ that is independent of θ. Given the ELBO, we also have:

$$\begin{aligned}
ELBO(\theta, Q(Y)) &= \mathbb{E}_{Q(Y)}[\log \frac{P(X, W, Y; \theta)}{Q(Y)}] \\
&= \mathbb{E}_{Q(Y)}[\log \frac{P(X, W, Y; \theta) P(Y|X, W; \theta)}{Q(Y) P(Y|X, W; \theta)}] \\
&= \mathbb{E}_{Q(Y)}[\log \frac{P(Y|X, W; \theta) P(X, W; \theta) P(Y|X, W; \theta)}{Q(Y) P(Y|X, W; \theta)}] \\
&= \mathbb{E}_{Q(Y)}[\log P(X, W; \theta) \frac{P(Y|X, W; \theta)}{Q(Y)}] \\
&= \mathbb{E}_{Q(Y)}[\log P(X, W; \theta)] - \mathbb{E}_{Q(Y)}[\frac{Q(Y)}{P(Y|X, W; \theta)}] \\
&= \log P(X, W; \theta) - \mathrm{KL}(Q(Y) || P(Y|X, W; \theta)).
\end{aligned} \tag{10}$$

Thus we can see that maximizing the ELBO is equivalent to maximizing $\log P(X, W; \theta)$ when $P(Y|X, W; \theta)$ is close to $Q(Y)$, i.e., the Kullback-Leibier divergence $\mathrm{KL}(Q(Y) || P(Y|X, W; \theta))$ is approaching to 0. Thus we take $Q(Y) = P(Y|X, Y; \theta^t)$ with current estimation θ^t from the model, and obtain Eq. (4).

A.2. Proof of Proposition 3.2

Proof. Applying the maximum log-likelihood estimation to the weak supervision dataset $\mathcal{D} = \{(\mathbf{x}_i^{1:L}, w_i)\}_{i \in [N]}$, where $w \in W$ is the weak supervision for each sequence input $\mathbf{x}^{1:L}$ with $L \geq 1$. When $L = 1$, $\mathbf{x}$ represents an individual training instance, otherwise it represents a group of sequence as discussed in the main paper. For simplicity, we consider L as a fixed value for $\mathcal{L}$ here, but in practice it can denote variable length. We have Assumption 3.1 that the predictions and precise labels in the sequence are conditionally independent given whole input sequence.

$$\begin{aligned}
&\arg\max_{\theta} \mathbb{E}_{Y|X, W; \theta^t}[\log P(X, W, Y; \theta)] \\
&= \arg\max_{\theta} \mathbb{E}_{Y|X, W; \theta^t}[\log P(W|Y, X; \theta) P(Y|X; \theta) P(X; \theta)] \\
&= \arg\max_{\theta} \mathbb{E}_{Y|X, W; \theta^t}[\log P(Y|X; \theta)] + \mathbb{E}_{Y|X, W; \theta^t}[\log P(W|Y, X; \theta)] \quad P(X) \text{ is independent of } \theta \\
&= \arg\max_{\theta} \mathbb{E}_{Y|X, W; \theta^t}[\log P(Y|X; \theta)] + \log P(W|Y, X; \theta) \quad P(W|Y, X; \theta) \text{ is fixed for any } P(Y|X, W; \theta^t)
\end{aligned} \tag{11}$$

The derived objective $\mathcal{L}_{\text{Weak}}$ on the dataset $\mathcal{D}$ from the EM formulation thus have two terms, where the first unsupervised term $\mathcal{L}_{\text{U}}$ corresponds to:

$$\begin{aligned}
\mathcal{L}_{\text{U}} &= \sum_{i=1}^{N} \mathbb{E}_{y_i^{1:L}|\mathbf{x}_i^{1:L}, w_i; \theta^t}[\log p(y_i^{1:L}|\mathbf{x}_i^{1:L}; \theta)] \\
&= \sum_{i=1}^{N} p(y_i^{1:L}|\mathbf{x}_i^{1:L}, w_i; \theta^t) \log \prod_{j=1}^{L} p(y_i^j|\mathbf{x}_i^j; \theta) \quad \text{Instance-level model} \\
&= \sum_{i=1}^{N} \sum_{j=1}^{L} p(y_i^j|\mathbf{x}_i^{1:L}, w_i; \theta^t) \log p(y_i^j|\mathbf{x}_i^j; \theta) \quad \text{Conditional independence in Assumption 3.1},
\end{aligned} \tag{12}$$

and the supervised term $\mathcal{L}_{\text{S}}$ as:

$$\mathcal{L}_S = \sum_{i=1}^{N} \log p(w_i|y_i^{1:L}, \mathbf{x}_i^{1:L}; \theta) \tag{13}$$

□

B. Method

B.1. Illustration of Possible Labelings as Trellis of Common Weak Supervision Settings

Here, we present more illustration of the expanded trellis from the NFA in Fig. 3. The demonstration of weak supervision is over a group of 4 instances for LProp and 2 instances for pairwise observations.

The trellis of LProp with exact two positive samples is shown in Fig. 7. Note that for LProp, the number of states in its NFA depends on the exact count from the weak supervision as discussed in the main paper. The unlabeled data with class prior information can also be represented as expected label count and uses the trellis representation of LProp.

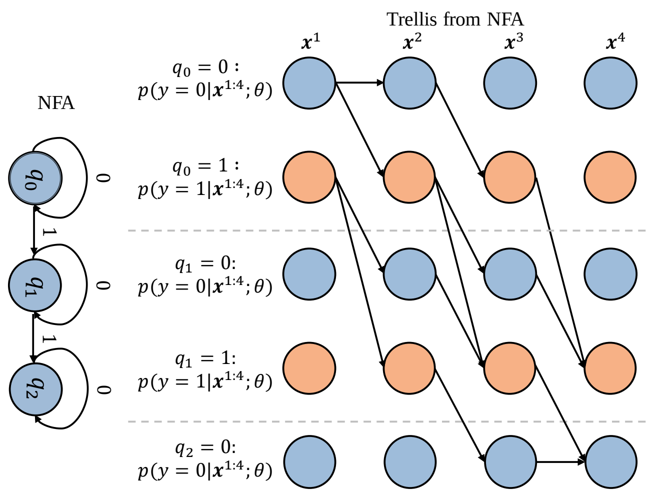

Figure 7. Illustration of trellis expanded from the NFA of label proportion on 4 instances whose weak supervision is exact two positive samples. We omit the last state of $q_2 = 1$ for simplicity because no path goes through it.

We also present the illustration of PComp, PSim, and PDsim in Fig. 8, Fig. 9(a), and Fig. 9(b) respectively. Although we use 3 states in their NFA, we instead directly use 4 states in the expanded trellis to represent all the labelings for pairwise observations, i.e., $\{(0,0), (1,1), (0,1), (1,0)\}$. Despite the notation difference, they represent the same weak supervision. SimConf and ConfDiff can also be represented similarly by weighting the path with confidence score and similarity score.

For totally unlabeled data, every symbol in $\mathcal{Y}$ can be allowed for transition, thus its trellis degenerate to the prediction probability of each instance.

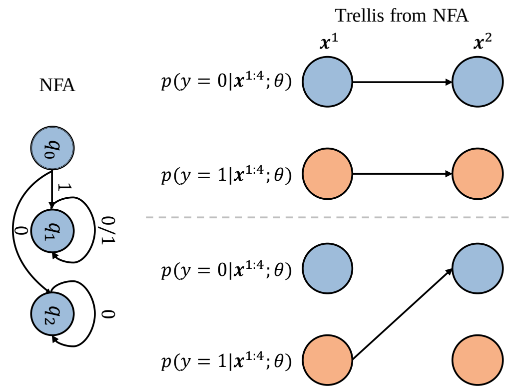

Figure 8. Illustration of trellis expanded from the NFA of pairwise comparison on 2 instances whose weak supervision is the first instance is more position than the second. We directly use 4 states to fully represent the cases $\{(0,0),(1,1),(0,1),(1,0)\}$, which might looks different from its NFA who has only 3 states, but they indicate the same weak supervision.

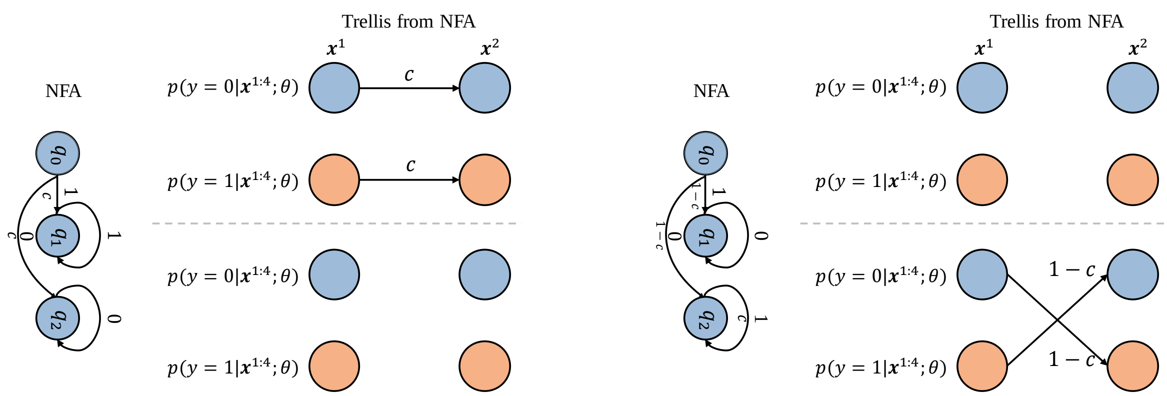

(a) Pairwise similarity (b) Pairwise dissimilarity

Figure 9. Illustration of trellis expanded from the NFA of (a) pairwise similarity and (b) pairwise dissimilarity on 2 instances whose weak supervision is the whether the pair has similar or dissimilar supervision. We directly use 4 states to fully represent the cases $\{(0,0),(1,1),(0,1),(1,0)\}$, which might looks different from its NFA who has only 3 states, but they indicate the same weak supervision. Similarity confidence and confidence different can also be represented using the trellis here by weighting each path according to the similarity or confidence score.

B.2. Pseudo-algorithm of the Forward-Backward Algorithm of Common Weak Supervision Settings

We present the pseudo-algorithm of performing the forward-backward algorithms on common weak supervision settings we evaluated. The pseudo-algorithm also corresponds to description of the trellis expanded from the NFA. Note that the only difference for each weak supervision setting is the NFA modeling. Once having the NFA modeling of weak supervision, the finite states and the transition between states are determined, and thus the forward-backward algorithm can be performed accordingly. We perform the forward-backward algorithm in log-space for numerical stability. Moreover, we use the log-sum-exp trick for computing the addition in log-space. For illustration simplicity, we present the pseudo-algorithm on single instance/group inputs and binary predictions, but in practice we implement the forward-backward pass at batch of instances/groups inputs and multi-class predictions. Here we illustrate the pseudo-algorithm for MultiIns in Algorithm 1, LProp in Algorithm 2, PComp in Algorithm 3, respectively. Other settings should either be similar or simple to solve.

Algorithm 1 Forward-Backward Algorithm for multiple instance (MultiIns) Learning

Require: Predicted probability in log-space as log_probs from $\mathbf{x}^{1:L}$, w with 0 for no positive and 1 for at least one positive in the bag, bag length as L.

Number of states as $Q \leftarrow 4$.
Initialize $\alpha \in \mathbb{R}^{2Q \times L}$ with $-1e12$ for forward pass.
$\alpha[0,0], \alpha[1,0] \leftarrow log\_probs[0,0], log\_probs[0,1]$.
for $i = 1$ to L **do**
  if $i < L - 1$ **then**
    Update $\alpha[0,i] = \alpha[0,i-1] + log\_probs[i,0]$.
  else
    Update $\alpha[0,i] = -1e12$.
  end if
  if $i \geq 2$ **then**
    Update $\alpha[2,i] = \alpha[1,i-1] + \alpha[2,i-1] + \alpha[3,i-1] + log\_probs[i,0]$.
    Update $\alpha[3,i] = \alpha[1,i-1] + \alpha[2,i-1] + \alpha[3,i-1] + log\_probs[i,1]$.
  else
    Update $\alpha[2,i] = \alpha[1,i-1] + log\_probs[i,0]$.
    Update $\alpha[3,i] = \alpha[1,i-1] + log\_probs[i,1]$.
  end if
end for
Compute forward probability $p(w|\mathbf{x}^{1:L}, y^{1:L}; \theta)$ from $\exp(\alpha)$ as sup_preds.
if w = 0 **then**
  $em\_targets = ones\_like(log\_probs)$
  Return sup_preds, $em\_targets$
end if
Initialize $\beta \in \mathbb{R}^{2Q \times L}$ with $-1e12$ for backward pass.
$\beta[1, L-1], \beta[2, L-1], \beta[3, L-1] \leftarrow log\_probs[L-1, 1], log\_probs[L-1, 0], log\_probs[L-1, 1]$.
for $i = L - 2$ down to 0 **do**
  $\beta[0,i] = \beta[0,i+1] + \beta[1,i+1] + log\_probs[i,0]$.
  $\beta[1,i] = \beta[2,i+1] + \beta[3,i+1] + log\_probs[i,1]$.
  if $i > 0$ **then**
    $\beta[2,i] = \beta[2,i+1] + \beta[3,i+1] + log\_probs[i,0]$.
    $\beta[3,i] = \beta[2,i+1] + \beta[3,i+1] + log\_probs[i,1]$.
  end if
end for
Adjust β based on log_probs.
$\gamma = \alpha + \beta$.
$\gamma = \exp(\gamma.transpose(0,1))$.
Compute joint probability $p(y^j|\mathbf{x}^{1:L}, w; \theta)$ as $em\_targets$
Return sup_preds, $em\_targets$

Algorithm 2 Forward-Backward Algorithm for label proportion (LProp) Learning

Require: Predicted probability in log-space as log_probs of $\mathbf{x}^{1:L}$, w indicates the count of positive instance.
Number of states $Q \leftarrow 2 \times w + 1$.
Initialize $\alpha \in \mathbb{R}^{Q \times L}$ with $-1e12$ for forward pass.
$\alpha[0, 0] \leftarrow log\_probs[0, 0]$.
if $count > 0$ **then**
    $\alpha[1, 0] \leftarrow log\_probs[0, 1]$.
end if
for $i = 1$ to L **do**
    Update $\alpha[0, i] = \alpha[0, i-1] + log\_probs[i, 0]$.
    if $count > 0$ **then**
        Update $\alpha[1, i] = \alpha[0, i-1] + log\_probs[i, 1]$.
    end if
    for $j = 2$ to Q **do**
        if $i < w - (Q - j)//2$ **then**
            Continue to next iteration of j.
        end if
        if j % 2 = 0 **then**
            Update $\alpha[j, i] = \alpha[j, i-1] + \alpha[j-1, i-1] + log\_probs[i, 0]$
        else
            Update $\alpha[j, i] = \alpha[j-1, i-1] + \alpha[j-2, i-1] + log\_probs[i, 1]$
        end if
    end for
end for
Compute forward probability sup_preds from $\exp(\alpha)$.
Adjust α based on w and Q to avoid underflow.
Initialize $\beta \in \mathbb{R}^{Q \times L}$ with $-1e12$ for backward pass.
Set initial values of $\beta[-1, -1]$ and $\beta[-2, -1]$ based on w.
for $i = b - 2$ down to 0 **do**
    if $i \geq w$ **then**
        $\beta[-1, i] = \beta[-1, i+1] + log\_probs[i, 0]$
    end if
    if $i \geq w \& w > 0$ **then**
        $\beta[-2, i] = \beta[-1, i+1] + log\_probs[i, 0]$
    end if
    for $j = 0$ to $k - 2$ **do**
        if $i < count - (k - j)//2$ **then**
            Continue to next iteration of j.
        end if
        if j % 2 = 0 **then**
            Update $\beta[j, i] = \beta[j, i+1] + \beta[j+1, i+1] + log\_probs[i, 0]$
        else
            Update $\beta[j, i] = \beta[j+1, i+1] + \beta[j+2, i+1] + log\_probs[i, 1]$
        end if
    end for
end for
Adjust β based on log_probs.
$\beta = \exp(\beta)$
$\gamma = \alpha + \beta$.
$\gamma = \exp(\gamma.transpose(0, 1))$.
Compute joint probability $p(y^j | \mathbf{x}^{1:L}, w; \theta)$ as $em\_targets$
Return sup_preds, $em\_targets$

Algorithm 3 Forward-Backward Algorithm for pairwise comparison (PComp) Learning

Require: Predicted probability in log-space as log_probs of $\mathbf{x}^{1:L}$.

1: Number of states $Q \leftarrow 4$.
2: Initialize $\log\_alpha \in \mathbb{R}^{4\times 2}$ with $-1e12$ for the forward pass.
3: $\alpha[0,0] = log\_probs[0,0]$
4: $\alpha[1,0] = log\_probs[0,1]$
5: $\alpha[3,0] = log\_probs[0,1]$
6: $\alpha[0,1] = \alpha[0,0] + log\_probs[1,0]$
7: $\alpha[1,1] = \alpha[1,0] + log\_probs[1,1]$
8: $\alpha[2,1] = \alpha[3,0] + log\_probs[1,0]$
9: Compute forward probability from $\exp(\alpha)$.
10: Initialize $\log\_beta \in \mathbb{R}^{4\times 2}$ with $-1e12$ for the backward pass.
11: $\beta[0,1] = log\_probs[1,0]$
12: $\beta[1,1] = log\_probs[1,1]$
13: $\beta[2,1] = log\_probs[1,0]$
14: $\beta[0,0] = \beta[0,1] + log\_probs[0,0]$
15: $\beta[1,0] = \beta[1,1] + log\_probs[0,1]$
16: $\beta[3,0] = \beta[1,2] + log\_probs[0,1]$
17: Adjust β based on repeated log_probs.
18: $\gamma = \alpha + \beta$.
19: $\gamma = \exp(\gamma.transpose(0,1))$.
20: Compute the EM targets $em\_targets$ from γ.
21: Return $em\_targets$, sup_preds

C. Experiments

In this section, we provide more details on the training setup and hyper-parameters for our evaluations. We also present the details on datasets and class split of the datasets. More results of other weak supervision settings can be found in Appendix C.6.

C.1. Datasets and Classes Splits

Table 6. Dataset details

Dataset	# Classes	# Training	# Validation	# Unlabeled
MNIST	10	60,000	10,000	-
F-MNIST	10	60,000	10,000	-
CIFAR-10	10	50,000	10,000	-
CIFAR-100	100	50,000	10,000	-
STL-10	10	5,000	8,000	100,000
ImageNet-100	100	130,000	5,000	-

The datasets details are shown in Table 6.

For some weak supervision settings, such as pairwise observations, positive unlabeled, and unlabeled unlabeled learning, we split the classes of each dataset into binary as follows.

MNIST. For multiple instance learning and label proportion learning, we set digit 9 as positive class, and others as negative class for binary classification. For other settings, we set digits 0-4 as positive class, and others as negative class.

F-MNIST. Similarly, for multiple instance learning and label proportion learning, we set the 9-th class as positive class. For other settings, we set the classes related to tops as positive class, i.e., $\{5, 7, 9\}$.

CIFAR-10 and STL-10. For multiple instance learning and label proportion learning, we set bird, i.e., class 3, as positive class. For other settings, we set transportation related classes as positive class, i.e., airplane, automobile, ship, truck.

CIFAR-100. Binary classification on CIFAR-100 is not conduced on multiple instance learning and label proportion learning. For other settings, we select the 40 animal related classes from 100 total classes as positive class.

C.2. Partial Labels

Here we provide more training details and results of partial label learning.

C.2.1. Setup

We follow RCR (Wu et al., 2022) for experiments of partial label learning. More specifically, we generate synthetic uniform partial label datasets, where we uniformly select each incorrect label for each instance into a candidate label set with partial ratio as probability. We adopt same training hyper-parameters for the baseline methods and GLWS for fair comparison. A summarize of training parameters is shown in Table 7.

Table 7. Hyper-parameters for partial label (PartialL) learning used in experiments.

Hyper-parameter	MNIST & F-MNIST	CIFAR-10	CIFAR-100	STL-10	ImageNet-100
Image Size	28	32	32	96	224
Model	LeNet-5	WRN-34-10	WRN-34-10	ResNet-18	ResNet-34
Batch Size	64	64	64	64	32
Optimizer	SGD	SGD	SGD	AdamW	AdamW
Learning Rate	0.1	0.1	0.1	0.001	0.001
Weight Decay	1e-4	1e-4	1e-4	1e-4	1e-4
LR Scheduler	MultiStep	MultiStep	MultiStep	Cosine	Cosine
Training Epochs	200	200	200	200	200

For MNIST and F-MNIST, we use LeNet-5 (LeCun et al., 1998). We adopt WideResNet-34-10 variant (Zagoruyko & Komodakis, 2016) for CIFAR-10 and CIFAR-100, ResNet-18 (He et al., 2016) for STL-10, and ResNet-34 for ImageNet-100.

Table 8. Accuracy on partial label (PartialL) learning. All results are averaged over three runs. This table is complementary to Table 1.

Dataset	MNIST				F-MNIST				CIFAR-10				CIFAR-100				STL-10		ImageNet-100	
Partial Ratio	0.10	0.30	0.50	0.70	0.10	0.300	0.50	0.70	0.10	0.30	0.50	0.70	0.01	0.05	0.10	0.20	0.10	0.30	0.01	0.05
CC	99.25±0.02	99.18±0.05	99.08±0.03	98.93±0.05	**91.44±0.16**	91.10±0.07	90.45±0.09	89.55±0.28	95.25±0.03	94.13±0.09	92.51±0.04	89.01±0.20	79.68±0.14	78.73±0.24	77.44±0.32	74.60±0.17	77.02±0.69	73.26±0.34	73.14±0.94	64.67±0.74
LWS	98.23±0.02	98.04±0.12	97.95±0.11	96.96±0.10	88.17±0.11	88.10±0.05	87.59±0.18	86.60±0.13	91.42±0.03	88.76±0.45	85.66±0.32	80.71±0.10	69.46±0.28	55.49±0.67	50.67±0.33	43.51±0.32	67.65±0.33	58.18±1.65	72.04±0.77	62.13±0.95
PRODEN	99.12±0.52	98.89±0.52	98.27±0.68	97.77±0.82	90.95±0.63	**91.96±0.70**	90.40±0.58	89.20±0.45	95.25±0.45	95.68±0.40	93.85±0.60	91.11±0.70	79.06±0.24	79.17±0.36	77.80±0.31	74.99±0.57	77.74±0.52	74.18±0.41	78.61±0.63	77.59±0.60
PiCO	99.22±0.01	99.20±0.01	99.10±0.02	98.96±0.09	90.30±1.44	91.41±0.05	90.42±0.14	89.73±0.21	95.37±0.12	95.14±0.16	93.32±0.23	90.26±0.20	79.49±0.13	78.71±0.18	77.50±0.15	74.89±0.13	77.44±0.26	73.19±1.05	80.93±0.81	78.74±1.34
RCR	99.25±0.04	99.21±0.04	99.11±0.03	99.01±0.05	91.26±0.17	91.26±0.08	90.82±0.12	90.06±0.03	95.57±0.19	94.65±0.05	94.04±0.02	91.45±0.10	79.89±0.23	78.93±0.30	78.03±0.07	75.40±0.12	78.02±0.40	74.67±0.56	81.52±0.94	79.67±1.22
GLWS	**99.25±0.01**	**99.28±0.05**	**99.12±0.02**	**99.14±0.04**	91.42±0.22	91.28±0.09	**90.85±0.10**	**90.35±0.15**	**95.61±0.03**	**95.23±0.11**	**94.31±0.09**	**92.06±0.14**	**80.06±0.17**	**79.47±0.09**	**78.35±0.11**	**75.82±0.25**	**78.56±0.27**	**74.79±0.21**	**82.66±0.54**	**81.09±0.50**

For optimizer, we use SGD (Loshchilov & Hutter, 2016) for MNIST, F-MNIST, CIFAR-10, CIFAR-100, and AdamW (Kingma & Ba, 2014) for STL-10 and ImageNet-100.

C.2.2. Results

We present more results on partial label learning in Table 8, where our method in general achieves the best performance.

C.3. Aggregate Observations

More details about experiments of aggregate observations are shown here.

C.3.1. Setup

For aggregate observation, the largest dataset previously experimented is MNIST, which is unpractical. Here we present the training hyper-parameters we used for MultiIns and LProp in Table 9.

Table 9. Hyper-parameters for multiple instance (MultiIns) and label proportion (LProp) learning used in experiments.

Hyper-parameter	MNIST & F-MNIST	CIFAR-10	CIFAR-100	STL-10	ImageNet-100
Image Size	28	32	32	96	224
Model	LeNet-5	WRN-28-2	ResNet-18	ResNet-18	ResNet-34
Batch Size	4	4	4	4	8
Optimizer	AdamW	AdamW	AdamW	AdamW	AdamW
Learning Rate	5e-4	1e-3	1e-3	1e-3	1e-3
Weight Decay	1e-4	5e-4	5e-4	5e-4	1e-4
LR Scheduler	Cosine	Cosine	Cosine	Cosine	Cosine
Training Epochs	100	100	100	100	100

We train all methods in both settings for 100 epochs and AdamW optimizer. We set the learning rate to 1e-4 for MNIST and F-MNIST, and 1e-3 for others. WideResNet-28-2 is utlized for CIFAR-10, while ResNet-18 is used for CIFAR-100 and STL-10. Since each training instance for aggregate observations is a group of examples of variable length, we set batch size to 4 universally or 8 for ImageNet-100.

To create aggregate observations, we sample instances from the dataset to form groups/bags according to the specified Gaussian distribution. Then we summarize the weak supervision as counts of the labels in the group. which eventually convert to flags of existence of positive samples for multiple instance learning. For binary classification, we ensure that the number of negative bags and positive bags are balanced.

C.3.2. Results

We present more results of the binary classification of aggregate observations on MNIST, F-MNIST, CIFAR-10 and STL-10 in Table 10. The multi-class classification results of MNIST and F-MNIST are also shown here. One can observe that, for both settings, our method is on par with Count Loss on MNIST and F-MNIST, and in general performs the best on multi-class classification settings of these two datasets. Moreover, on binary classification of CIFAR-10 and STL-10, our method also outperforms the baselines.

C.4. Pairwise Observations

We provide more training details and results of pairwise observations here.

Table 10. Accuracy on both binary and multi-class multi-label aggregate observations of multiple instance (MI) learning and label proportion (LP) learning. All results are averaged over three runs. This table is complementary to Table 2.

Dataset	MNIST				F-MNIST				CIFAR-10		STL-10	
# Classes	2		10		2		10		2		2	
Dist # Bags	$\mathcal{N}(10,2)$ 1,000	$\mathcal{N}(50,10)$ 250	$\mathcal{N}(10,2)$ 1,000	$\mathcal{N}(20,5)$ 500	$\mathcal{N}(10,2)$ 1,000	$\mathcal{N}(50,10)$ 250	$\mathcal{N}(10,2)$ 1,000	$\mathcal{N}(20,5)$ 500	$\mathcal{N}(10,2)$ 5,000	$\mathcal{N}(20,5)$ 2,500	$\mathcal{N}(5,1)$ 2,000	$\mathcal{N}(10,2)$ 1,000
Multiple Instance Learning												
Count Loss	**97.05**±0.45	91.21±0.46	**97.61**±0.20	**94.90**±0.24	**97.64**±0.10	91.62±1.96	**86.24**±0.33	82.02±0.06	**63.07**±1.63	56.71±2.23	57.90±6.11	51.50±1.65
UUM	81.08±0.11	74.00±0.53	63.96±5.39	23.43±4.01	91.40±1.00	87.38±1.32	64.24±2.28	28.57±5.90	58.25±1.59	57.67±0.61	57.05±4.94	57.60±0.64
GLWS	97.04±0.38	**91.54**±0.54	97.57±0.06	94.80±0.27	97.59±0.16	**93.21**±1.74	86.22±0.18	**82.05**±0.20	62.63±1.73	**57.94**±2.11	**58.40**±3.11	**58.03**±0.73
Label Proportion Learning												
LLP-VAT	98.18±0.19	92.37±2.15	98.21±0.07	**98.41**±0.10	98.13±0.10	96.83±0.11	86.99±0.45	83.65±0.94	85.33±0.44	54.20±2.72	50.51±0.36	50.15±0.21
Count Loss	**98.89**±0.21	96.46±0.19	97.95±0.02	98.29±0.11	**98.27**±0.12	**97.44**±0.16	87.50±0.05	85.70±0.54	89.46±0.24	67.58±2.03	65.93±0.91	56.23±1.15
UUM	-	-	-	-	-	-	-	-	-	-	61.54±2.16	-
GLWS	98.62±0.18	**97.05**±0.13	**98.42**±0.11	98.39±0.08	98.18±0.02	97.40±0.12	**88.02**±0.23	**86.20**±0.66	**89.77**±0.45	**68.03**±2.41	**66.04**±0.64	**58.20**±1.03

Table 11. Hyper-parameters for pairwise comparison (PComp), pairwise similarity (PSim), similarity confidence (SimConf), and confidence difference (ConfDiff) learning used in experiments.

Hyper-parameter	MNIST & F-MNIST	CIFAR-10	CIFAR-100	STL-10
Image Size	28	32	32	96
Model	LeNet-5	WRN-28-2	ResNet-18	ResNet-18
Batch Size	64	64	64	32
Optimizer	AdamW	AdamW	AdamW	AdamW
Learning Rate	5e-4	1e-3	1e-3	1e-3
Weight Decay	1e-4	1e-3	1e-3	1e-3
LR Scheduler	Cosine	Cosine	Cosine	Cosine
Training Epochs	100	100	100	100

Table 12. Accuracy on pairwise comparison (PComp) learning for binary classification. All results are averaged over three runs.

Dataset	F-MNIST			MNIST			CIFAR-10			CIFAR-100			STL-10		
#Pairs	25,000			25,000			20,000			20.000			5,000		
Prior	0.2	0.5	0.8	0.2	0.5	0.8	0.2	0.5	0.8	0.2	0.5	0.8	0.2	0.5	0.8
PComp ABS	92.82±0.89	99.73±0.04	90.96±0.74	91.54±0.86	96.86±0.30	91.09±1.08	88.75±0.60	91.78±0.10	87.37±1.89	73.10±0.15	81.67±0.24	66.06±1.19	78.38±0.50	79.07±0.40	56.45±1.86
PComp ReLU	99.65±0.07	99.73±0.08	98.41±0.41	90.30±0.28	96.71±0.10	92.87±0.22	90.47±0.94	92.18±0.22	90.57±0.21	73.10±0.77	81.77±0.59	66.57±1.27	**79.30**±0.85	79.68±0.75	67.01±1.71
PComp Teacher	92.41±0.38	93.92±0.81	92.54±0.15	92.79±0.45	93.03±0.93	91.46±1.31	92.29±0.19	93.33±0.38	91.35±0.27	72.72±0.33	78.59±0.60	67.43±3.09	78.09±0.68	77.33±0.14	72.88±0.15
PComp Unbiased	87.64±0.28	89.30±0.35	81.16±1.20	76.23±1.56	84.35±0.74	78.81±2.32	88.13±0.29	91.71±0.48	88.22±0.58	66.02±0.97	67.80±0.07	60.86±2.19	76.85±0.57	77.46±0.19	71.60±0.95
Rank Pruning	90.32±1.10	91.93±0.41	89.99±0.98	90.56±0.27	91.59±1.31	90.44±0.69	92.98±0.30	93.98±0.40	91.97±0.27	73.81±1.21	78.90±0.48	71.51±0.73	78.39±0.33	77.89±0.42	73.62±1.38
GLWS	**99.59**±0.01	**99.85**±0.02	**99.82**±0.03	**95.95**±0.15	**97.70**±0.11	**96.03**±0.39	**93.46**±0.32	**94.15**±0.10	**93.28**±0.38	**80.33**±0.07	**83.15**±0.16	**80.50**±0.20	79.15±0.78	**81.26**±0.54	**79.24**±0.87

C.4.1. SETUP

For pairwise observations $(\mathbf{x}^1), \mathbf{x}^2)$, we adopt the same training parameters for the four settings we evaluated, as shown in Table 11.

For PComp, PSim, and SimConf of class prior p, we form the pair observations by sampling from all positive pairs following p^2, all negative pairs following $(1-p)^2$, and positive and negative pairs following $2p(1-p)$, as in Feng et al. (2021); Wei et al. (2023); Cao et al. (2021b). For ConfDiff, we sample each instance in the pair independently according to the class prior p, as in Wang et al. (2023a). For PComp, the weak supervision is that $\mathbf{x}^1$ is more positive than $\mathbf{x}^2$. For PSim, the weak supervision is that the pairs are either similar or dissimilar. For SimConf and ConfDiff, we need pre-trained models to compute the similarity score as in (Cao et al., 2021b) and Wang et al. (2023a) respectively. We set two pre-trained models. The first one is the same architecture shown in Table 11, trained on a separate set of instances in each dataset and used to compute the score for the sampled pairs. The second one is CLIP models (Radford et al., 2021), where we compute the scores in a zero-shot manner.

C.4.2. RESULTS

We present more results of PComp in Table 12, PSim in Table 13, SimConf in Table 14, and ConfDiff in Table 15. Our method consistently and universally achieves the best performance on these settings in general.

Table 13. Accuracy on pairwise similarity (PSim) learning for binary classification. All results are averaged over three runs.

Dataset	F-MNIST			MNIST			CIFAR-10			CIFAR-100			STL-10		
#Pairs	30,000			30,000			25,000			25.000			5,000		
Prior	0.2	0.4	0.6	0.2	0.4	0.6	0.2	0.4	0.6	0.2	0.4	0.6	0.2	0.4	0.6
RiskSD	99.34±0.17	98.11±0.11	98.44±0.45	94.00±0.61	89.31±0.65	89.41±0.58	89.68±0.67	85.78±1.70	85.61±1.34	69.56±3.00	70.41±0.21	64.26±3.81	77.42±0.94	74.15±3.27	69.35±0.32
UUM	99.94±0.01	**99.93±0.01**	**99.93±0.01**	**99.04±0.08**	**99.12±0.05**	99.04±0.13	96.96±0.20	97.24±0.23	97.16±0.24	**86.95±0.08**	87.13±0.40	85.19±2.45	85.23±1.06	83.55±0.80	83.64±0.25
GLWS	**99.94±0.01**	**99.93±0.01**	**99.93±0.01**	98.96±0.01	99.07±0.01	**99.05±0.10**	**97.09±0.04**	**97.44±0.07**	**97.18±0.22**	86.89±0.42	**87.25±0.16**	**86.96±0.33**	**86.36±1.60**	**84.81±0.60**	**85.19±0.26**

Table 14. Accuracy on similarity confidence (SimConf) learning for binary classification. All results are averaged over three runs.

Dataset	F-MNIST				MNIST				CIFAR-10				CIFAR-100				STL-10			
#Pairs	30,000				30,000				25,000				25.000				5,000			
Conf Model	LeNet-5		CLIP ViT-B-16		LeNet-5		CLIP ViT-B-16		WRN-28-2		CLIP ViT-B-16		ResNet-18		CLIP ViT-B-16		ResNet-18		CLIP ViT-B-16	
Prior	0.5	0.7	0.5	0.7	0.5	0.7	0.5	0.7	0.4	0.6	0.4	0.6	0.4	0.6	0.4	0.6	0.4	0.6	0.4	0.6
Sconf Abs	99.03±0.01	99.63±0.09	98.16±0.11	99.11±0.29	98.39±0.24	96.47±0.11	75.28±0.91	76.91±1.04	87.36±1.22	89.36±0.82	90.16±1.32	88.97±0.12	75.79±0.27	76.79±0.21	69.51±0.44	63.39±0.30	76.84±0.75	76.50±0.68	74.44±0.78	66.33±1.87
Sconf ReLU	99.45±0.04	99.65±0.08	98.02±0.09	**99.11±0.30**	98.23±0.15	96.40±0.16	76.14±0.11	76.91±1.05	88.56±0.57	89.66±0.36	90.50±0.44	88.79±0.41	74.95±0.55	76.83±0.62	69.67±1.51	63.77±2.05	77.40±0.31	76.51±0.71	75.26±0.66	67.12±2.08
Sconf NN Abs	99.63±0.10	99.48±0.10	98.51±0.03	99.19±0.25	98.41±0.06	96.32±0.10	76.42±0.45	77.57±0.73	89.04±0.88	88.97±0.29	89.05±2.11	87.76±0.82	74.55±0.23	75.82±0.44	68.93±2.00	63.79±1.43	77.55±0.31	75.97±0.66	75.66±0.51	65.80±0.45
Sconf Unbiased	99.15±0.07	99.64±0.06	98.44±0.03	99.16±0.33	98.05±0.05	95.98±0.45	76.38±0.13	77.37±0.90	88.72±0.52	87.90±0.47	88.71±0.59	88.86±0.25	72.87±1.30	73.23±1.23	69.55±0.31	64.51±2.88	77.76±0.40	76.74±0.63	74.36±0.60	67.42±2.06
GLWS	**99.90±0.00**	**99.89±0.01**	**98.67±0.30**	98.55±0.08	**98.58±0.03**	**98.48±0.03**	**76.78±0.21**	**78.47±0.18**	**95.97±0.11**	**95.93±0.02**	**97.88±0.11**	**97.60±0.13**	**85.58±0.88**	**87.85±0.49**	**87.94±0.34**	**86.56±0.94**	**78.64±0.16**	**78.33±0.07**	**79.06±0.05**	**78.69±0.08**

Table 15. Accuracy on confidence difference (ConfDiff) learning for binary classification. All results are averaged over three runs.

Dataset	F-MNIST				MNIST				CIFAR-10				CIFAR-100				STL-10			
#Pairs	30,000				30,000				25,000				25.000				5,000			
Conf Model	LeNet-5		CLIP ViT-B-16		LeNet-5		CLIP ViT-B-16		WRN-28-2		CLIP ViT-B-16		ResNet-18		CLIP ViT-B-16		ResNet-18		CLIP ViT-B-16	
Prior	0.5	0.7	0.5	0.7	0.5	0.7	0.5	0.7	0.4	0.6	0.4	0.6	0.4	0.6	0.4	0.6	0.4	0.6	0.4	0.6
ConfDiff Abs	99.82±0.03	99.36±0.14	98.90±0.36	93.80±1.16	97.31±0.08	92.11±3.31	91.67±0.91	89.19±2.26	90.12±4.19	93.18±0.42	88.61±7.50	94.11±0.29	82.89±0.32	81.80±1.95	81.45±0.26	80.64±1.33	73.17±2.06	73.53±3.19	77.33±0.74	76.72±0.57
ConfDiff ReLU	99.83±0.03	99.31±0.18	99.29±0.11	95.54±1.07	97.42±0.11	93.28±2.35	90.26±0.76	88.97±1.43	90.36±3.07	93.05±0.31	88.78±2.91	93.86±0.48	83.13±0.27	82.64±1.05	81.68±0.46	80.75±1.03	72.39±3.06	73.41±1.83	77.59±0.17	76.11±1.54
ConfDiff Unbiased	99.83±0.04	99.31±0.21	99.43±0.10	97.59±0.27	97.34±0.09	94.46±1.86	89.22±1.39	88.05±0.68	90.05±5.23	93.23±0.33	87.91±9.03	93.87±0.38	83.65±0.11	82.69±1.08	81.94±0.43	80.89±0.88	72.13±2.70	73.53±3.19	77.98±0.08	77.81±0.40
GLWS	**99.88±0.01**	**98.43±0.33**	**99.86±0.01**	**99.42±0.09**	**98.30±0.05**	**97.74±0.07**	**93.41±0.12**	**91.88±0.08**	**95.36±0.19**	**94.81±0.03**	**96.14±0.67**	**96.23±0.11**	**86.12±0.76**	**84.95±1.20**	**83.42±1.12**	**82.53±0.27**	**77.99±0.75**	**76.24±0.42**	**78.49±0.31**	**78.57±0.28**

C.5. Unlabeled Data

C.5.1. SETUP

Table 16. Hyper-parameters for positive unlabeled (PosUlb), unlabeled unlabeled (UlbUlb), and similarity dsimilarity unlabeled (SimDsimUlb) learning used in experiments.

Hyper-parameter	MNIST & F-MNIST	CIFAR-10	CIFAR-100	STL-10
Image Size	28	32	32	96
Model	LeNet-5	WRN-28-2	ResNet-18	ResNet-18
Batch Size	64	64	64	32
Optimizer	AdamW	AdamW	AdamW	AdamW
Learning Rate	5e-4	1e-3	1e-3	1e-3
Weight Decay	1e-4	1e-3	1e-3	1e-3
LR Scheduler	Cosine	Cosine	Cosine	Cosine
Training Epochs	50	50	50	50

For unlabeled data, we evaluate on PosUlb, UlbUlb, and SDUlb settings with class priors. The hyper-parameters are shown in Table 16. For PosUlb, we sample labeled set from only positive samples, and form the unlabeled set with both positive and negative samples whose distribution follows the class prior. For UlbUlb, we form both unlabeled set similarly as in PosUlb. For SDUlb, the labeled pairwise observation is formed similarly as in PSim.

C.5.2. RESULTS

We present more results of PosUlb in Table 17, and evaluation on UlbUlb and SDUlb in Table 18 and **??** respectively. Our approach achieves the best results across different settings except on F-MNIST of UlbUlb evaluation.

C.6. Other Settings

Here we present the evaluation of other weak supervision settings.

C.6.1. POSITIVE CONFIDENCE LEARNING

We evaluation on positive confidence (PosConf) learning (Ishida et al., 2018), where the weak supervision is given as the confidence score of a sample being positive, from the pre-trained models. The NFA of PosConf consists of L states for

Table 17. Accuracy on positive unlabeled (PU) learning for binary classification. All results are averaged over three runs.

	FMNIST			MNIST			CIFAR-10			CIFAR-100			STL-10		
Prior	0.3			0.5			0.4			0.4			0.4		
# Pos	100	500	1000	100	500	1000	500	1000	2000	1000	2000	4000	500	1000	2000
Count Loss	99.48±0.25	99.72±0.01	99.77±0.02	85.25±0.53	93.27±0.65	95.14±0.49	87.76±0.59	88.61±0.68	87.96±0.42	70.57±1.50	78.13±0.19	78.17±2.49	77.11±0.60	78.79±0.96	79.77±1.40
CVIR	97.77±0.98	99.24±0.22	99.31±0.37	74.67±1.83	93.61±1.08	95.95±0.26	88.65±2.59	93.37±0.24	94.69±0.24	78.56±0.22	82.94±0.37	85.22±1.07	77.67±1.11	81.84±1.10	85.38±0.83
Dist PU	96.87±0.24	97.23±0.31	97.44±0.15	85.60±1.69	90.94±1.87	95.36±0.38	83.61±4.52	82.60±2.48	85.38±1.13	69.12±1.39	69.83±1.43	70.82±1.12	71.07±1.12	70.89±0.63	69.86±1.07
NN PU	95.27±1.40	98.63±0.54	99.18±0.10	67.99±0.80	77.84±0.35	78.77±1.50	87.45±0.66	90.32±0.50	86.60±1.26	75.49±0.88	77.26±0.47	78.53±0.95	74.57±0.54	77.32±0.95	77.68±2.07
U PU	85.09±0.53	84.90±0.26	84.85±0.43	74.56±0.79	79.58±1.27	79.41±0.16	81.38±2.17	87.51±0.24	90.54±0.11	68.70±0.79	70.08±0.98	74.07±1.51	73.37±0.57	75.31±0.74	79.08±0.76
Var PU	95.02±0.02	97.52±1.48	99.22±0.26	48.61±0.64	48.61±0.01	51.22±2.88	77.00±2.82	84.45±2.58	87.34±1.80	61.02±0.22	66.02±0.29	70.57±1.94	60.98±0.78	62.37±1.44	62.18±1.02
GLWS	**99.55±0.21**	**99.84±0.03**	**99.87±0.01**	**87.57±0.21**	**95.04±0.74**	**96.85±0.17**	**91.67±0.19**	**93.69±0.28**	**94.80±0.12**	**80.30±0.12**	**83.32±0.23**	**85.98±0.29**	**79.60±0.95**	**82.87±0.83**	**87.51±0.60**

Table 18. Accuracy on unlabeled unlabeled (UU) learning for binary classification. All results are averaged over three runs.

	FMNIST			MNIST			CIFAR-10			CIFAR-100			STL-10		
# Ulb (Prior1, Prior2)	10,000 (0.4, 0.6)	30,000 (0.4, 0.6)	30,000 (0.8, 0.2)	10,000 (0.4, 0.6)	30,000 (0.4, 0.6)	30,000 (0.8, 0.2)	10,000 (0.4, 0.6)	25,000 (0.4, 0.6)	25,000 (0.8, 0.2)	10,000 (0.4, 0.6)	25,000 (0.4, 0.6)	25,000 (0.8, 0.2)	2,500 (0.4, 0.6)	5,000 (0.4, 0.6)	5,000 (0.8, 0.2)
UU Learn	**99.08±0.21**	**99.54±0.05**	**99.89±0.02**	89.75±0.41	93.24±1.02	98.19±0.10	88.32±1.64	89.42±0.11	94.46±0.05	66.23±1.59	66.37±3.05	71.23±0.54	78.59±1.97	72.55±1.27	81.42±1.31
GLWS	97.65±0.75	96.10±0.75	99.87±0.01	**97.27±0.24**	**96.87±0.80**	**98.91±0.04**	**94.45±0.45**	**95.01±0.44**	**98.07±0.07**	**74.66±1.29**	**76.75±3.05**	**89.83±0.44**	**82.09±2.33**	**84.78±1.19**	**88.27±0.96**

Table 19. Accuracy on similarity dissimilarity unlabeled (SDUlb) learning for binary classification. All results are averaged over three runs.

	FMNIST			MNIST			CIFAR-10			CIFAR-100			STL-10		
# Sim Pair	0	5,000	10,000	0	5,000	10,000	0	5,000	10,000	0	5,000	10,000	0	1,000	2,000
# Dsim Pair	10,000	5,000	0	10,000	5,000	0	10,000	5,000	0	10,000	5,000	0	2,000	1,000	0
# Ulb	20,000	20,000	20,000	20,000	20,000	20,000	20,000	20,000	20,000	20,000	20,000	20,000	4,000	4,000	4,000
RiskSD	87.61±0.48	89.32±0.15	87.06±0.97	87.18±0.10	89.09±1.89	83.02±1.24	78.69±3.56	84.61±0.50	79.09±2.36	65.36±0.28	65.87±1.23	63.43±1.45	66.94±1.42	66.92±2.86	65.02±1.59
GLWS	**92.81±0.08**	**92.57±0.24**	**92.24±1.20**	**97.27±0.11**	**96.54±0.36**	**96.41±0.95**	**93.12±0.28**	**92.76±0.82**	**84.24±1.20**	**78.59±1.32**	**73.02±1.54**	**70.24±1.16**	**79.28±0.98**	**75.93±1.69**	**75.67±1.26**

each instances in the training batch, and allows transition via both 0 and 1. Each positive transition path is weighted by the positive confidence score c, and each negative transition path is weighted by $1 - c$. This modeling can also be easily extended to subset confidence learning (Cao et al., 2021a) and soft label learning (Ishida et al., 2022).

The training parameters follow Table 11 and the results are shown in Table 20. Our method outperforms the baseline PConf (Ishida et al., 2018) except on MNIST.

Table 20. Accuracy on positive confidence (PosConf) learning for binary classification. All results are averaged over three runs.

Dataset	MNIST			F-MNIST			CIFAR-10			CIFAR-100		
# Data	15,000	30,000	30,000	15,000	30,000	30,000	10,000	25,000	25,000	10,000	25,000	25,000
Conf Model	LeNet-5	LeNet-5	CLIP ViT-B-16	LeNet-5	LeNet-5	CLIP ViT-B-16	WRN-28-2	WRN-28-2	CLIP ViT-B-16	ResNet-18	ResNet-18	CLIP ViT-B-16
PConf	**79.61±0.65**	**80.55±0.84**	**80.23±0.84**	91.25±0.23	90.67±0.13	91.10±0.13	90.71±1.86	92.74±0.26	92.70±0.22	74.09±1.61	79.39±0.50	79.49±0.62
GLWS	79.52±0.56	80.09±0.36	79.89±0.56	**92.22±0.06**	**91.95±0.16**	**92.05±0.09**	**95.31±0.13**	**96.84±0.12**	**96.93±0.14**	**83.70±0.13**	**86.62±0.18**	**87.24±0.13**